

Electrohydrodynamic instabilities observed in a nematic phase under oblique boundary conditions^{a)}

Dan Igner and Jack H. Freed

Baker Laboratory of Chemistry, Cornell University, Ithaca, New York 14853
(Received 29 December 1981; accepted 24 February 1982)

Electrohydrodynamic instabilities in the nematic phase of Merck "Phase V" with oblique boundary conditions were optically observed with a polarizing microscope in 25–100 μm "sandwich" cells. Oblique anchoring of the nematic was achieved by oblique evaporation of SiO on the plates. Two types of cells were used having the respective in-plane projection of the direction of evaporation on the two plates either parallel (p -type cells), or antiparallel (a -type cells). The low voltage dc instability observed for the p -type cells forms in an almost regular hexagonal pattern. By gradually increasing the voltage, the dc instability observed for the a -type cells forms at first as flows which originate at order disturbances created at imperfections in the SiO coating. Voltage increase causes these flows to detach themselves from the places of the imperfections and move solitarily. The moving flows are associated with what appears to be moving tilt inversion deformations (of splay-bend type) extending from the central part of the flow to some distance from it. When the voltage is further increased, a repeated process of replication of the flows, occurring on the associated tilt inversion deformations, leads to the creation of a periodic grid of moving flows. Other observed types of static and dynamic patterns under ac and dc excitation are reported, in particular: different types of cross rolls (ac conduction regime); variations of a pattern of what appears to be walls associated with flows, exhibiting an approximate wave number dependence on the electric field $k \sim E$; a striped pattern associated with what appears to be twist walls and the propagating interference patterns associated with their oscillations; a toroidal flow (sometimes associated with closed inversion walls) which creates and carries along closed nematic threads (dc regime); a polygonal grid of turbulent flows (dc regime); a flow pattern correlated with the movement of the moving chevron pattern; a cellular fast turn-off pattern related to the chevron pattern. This cellular pattern appears at first as moving snakelike regions in the chevron pattern which are bordered by disclination lines. Some features of dark, spotlike figures appearing on the chevron pattern are described. Preliminary interpretations of some of the observations are offered.

I. INTRODUCTION

Electrohydrodynamic instabilities (EHD) in nematics have been the object of many experimental and theoretical studies since the observation by Williams¹ of a striped pattern of lines when a sufficient voltage is applied to a thin (50–200 μm) layer of nematic between conducting glass plates.²

A model based on simplified assumptions which explains the formation of the instability seen by Williams has been given by Helfrich³ for dc excitation. This model has been extended to ac excitation, more general assumptions, and to related instabilities notably by the Orsay group⁴ and by others.⁵

There is now a generally accepted classification of the EHD in nematics according to the applied frequency in relation to relaxation times determined by mechanical, hydrodynamic, and electric constants of the nematics. Broadly, one distinguishes three regimes of EHD in nematics: the dc regime, the ac conduction regime, and the ac dielectric regime.

The dc-EHD in nematics are similar to the ones observed in dielectric isotropic liquids, in the sense that the mechanism for their formation involves charge injection (i. e., catalytic formation at one electrode of ions having the same sign as the electrode, cf. Refs. 6). A model which explains the EHD in isotropic dielectric liquids and which gained wide acceptance was proposed by Felici.^{6(a)} According to this model, the charge drift

conduction at low electric fields in dielectric liquids is replaced at high enough fields and in the presence of charge injection by a more effective mechanism involving flow loops. These loops of liquid flow carry the charge at speeds greater than the ionic drift under the field. The loops are set into motion by the drag the charges exert on the liquid in the presence of the electric field. The initiation of this flow instability could happen because of fluctuations or spatial irregularities in the injected charge. According to this model, in the case of weak unipolar injection, the first half of the liquid flow loop brings the injected charges to the other electrode, and the second half carries back the electrically neutral liquid to the injecting electrode.

The mechanism leading to the ac regime EHD's is specific to anisotropic fluids. As first realized by Carr,⁷ in the presence of distortions, the anisotropy of the conduction existing in nematics, can cause space charge formation, even from equal numbers of opposite charged ions. Under the forces exerted by the electric field, these space charges can drag the liquid into motion. As shown by Helfrich,³ loop flow instabilities not involving charge injection thus become possible in those cases in which the flows tend to enhance the space charge inducing distortions (which in turn enhance the flow). A process like this, in which nematic distortions (permanent or fluctuating) allow better conduction (of whatever type) and are in turn enhanced by this conduction, is called focalization. (Different authors use the term "focalization" with slightly different meanings.) As shown by the Orsay Liquid Crystal group,⁴ the Carr-Helfrich type of loop flows can persist even

^{a)}Supported by NSF Grant #DMR-81-02047.

under ac excitation, up to a cutoff frequency (of the order of tens to hundreds of cycles in a typical nematic having an ac conductivity of 10^{-10} – 10^{-9} mho cm^{-1}). This type of loop flow instability, not necessitating injection, and involving the Carr–Helfrich focalization mechanism, is classified as an ac conduction regime type of EHD. (The Williams domains are in this category.) Such EHD's are characterized by a threshold voltage (not dependent on the sample thickness), and the flows usually appear in the form of parallel rolls of a period comparable to the sample thickness. These instabilities can be formed in nematics possessing dielectric and conductivity anisotropies of opposite sign only.⁸

The ac dielectric regime, which can appear at frequencies higher than the cutoff frequency for the ac conducting regime is characterized by a threshold field (as opposed to the threshold voltage for the conduction regime). This field is proportional to the square root of the frequency. This kind of instability was first observed by Heilmeier and Helfrich,⁹ who also suggested that they are due to a parametric excitation of a bending oscillation in the nematic. A detailed theory given later by the Orsay group⁴ explains these instabilities as a periodic deformation of the nematic (created by the oscillations of a periodic charge distribution) under the parametric excitation of the ac field (See, however, Refs. 10). The amplitudes of the charge and associated mass flow oscillations are small compared to the sample thickness (no flow loops are formed). The distortion pattern has a periodicity of a few μm , not related to the sample thickness. Viewed with a polarizing microscope, the corresponding EHD pattern usually has the appearance of thin striations which could also be distorted into a "chevron" pattern.^{2,4(c)} While the dc and ac conduction instabilities which are related to flow loops require a relatively long time to be set on or off (tenths of a second to hours), the ac dielectric instabilities require only a few ms or less. (Because of this, they were called fast turnoff modes by Heilmeier and Helfrich.)

After it was discovered in the early 1970's that it is possible to prepare the sample plates for tilted anchoring of the nematics by using oblique evaporation of materials such as SiO, gold, etc. on the plates,¹¹ new patterns of EHD in nematics have been observed, notably instabilities in which the director no longer remains in the plane determined by the applied electric field and the direction of the alignment existing before the electric field is applied.^{12(a),12(b)}

In his basic paper in which he proposed that some nematics with molecules possessing wedge or crescent shapes can be piezoelectric, Meyer^{13(a)} showed that a nonanchored initially planar-oriented nematic layer held under an electric field between two flat electrodes can form a striped instability with stripes transverse to the initial director orientations (and with period $\propto E^{-1}$). He suggested that piezoelectricity could be the mechanism of formation of the Williams domains. A treatment for the anchored case was later given by Bobylev and Pikin.^{13(b)} It predicts longitudinal stripes (i.e., parallel to the initial director orientation). For parameters relevant to the present work their model predicts $\lambda \sim E^{-1}$

too. The liquid crystal piezoelectricity (better known today as flexoelectricity⁸) is a property of some liquid crystals which show polarization when deformed under a torque or conversely show curvature strains when polarized by electric fields.

Although the Williams domains and other related instabilities have by now been shown to have an electrohydrodynamic origin, a striped pattern instability first seen by Vistin^{14(a)} in thin ($\sim 10 \mu\text{m}$) samples of low conductance is believed to be a flexoelectric instability.^{14(b)} While the flexoelectric instabilities are not associated with mass flows, there are other instabilities showing an approximate E^{-1} dependence of the period which are associated with flows. One of these instabilities is the variable grid mode first described by Greubel and Wolff for thin samples ($< 10 \mu\text{m}$) of negative dielectric anisotropy.¹⁵ An EHD analog of the Williams domains, seen in a nematic obliquely anchored at the plates has also a $\lambda \sim E^{-1}$ dependence.^{12(a),12(b)} Another approximate $\lambda \propto E^{-1}$ instability was studied by Carr and collaborators in thick samples ($> 100 \mu\text{m}$, usually over 1 mm) of negative dielectric anisotropy nematics.^{16(a)–16(c)} Although the question whether there is a relation between instabilities of Refs. 15 and 16 has been raised,^{16(b),16(c)} it apparently has never been thoroughly investigated. Carr explains the instability he observed in the conduction regime at voltages which are normally high enough to destroy the Williams domains, as being caused by the accumulation of ionic charges on "defect" walls (distortion walls). These defect walls are created in regions of the greatest velocity flow of a Carr–Helfrich instability, which tends to form immediately after the field is applied. The charges are accumulated in the distortion walls because of the conduction anisotropy and interact with the field to create a shear flow which orients the nematic between the walls more toward the perpendicular to the electrodes.^{16(d)} Carr^{16(a)} and Carr *et al.*^{16(c)} suggest that the mechanism involved in the creation of the walls has a role to play in the turbulent regime called the "dynamic scattering mode"¹⁷ which appears when the Williams domains are destroyed at higher voltages.

The aim of the present paper is to report on a number of static and dynamic EHD patterns we have observed in the nematic phase of Merck "Phase V" in "sandwich geometry" samples prepared for oblique nematic anchoring of the plates with an obliquely evaporated $\sim 100 \text{ \AA}$ SiO coating, over frequencies of 0–300 Hz. Some of the patterns we report for phase V show features not reported in previous studies of other nematics in similar or related experiments. We also attempt to provide preliminary interpretations of our observations whenever possible.

II. EXPERIMENTAL

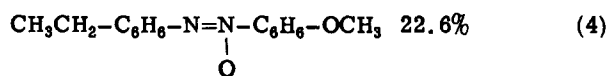
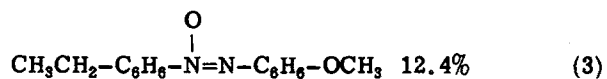
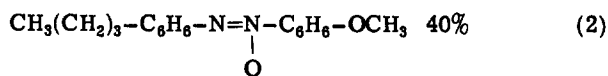
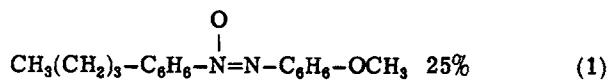
The 3×1 cm plates for the sandwich cell samples were cut out from 0.50 mm thick Nesatron "conducting glass" (supplied by PPG Industries, Pittsburgh, PA). The cleaning of the plates was done by washing in a weak Alconox solution with subsequent rinsing in distilled water, dipping in isopropyl alcohol and finally pressing dry between Kimwipe tissues. SiO was

obliquely evaporated on the conducting side of the plates in a vacuum of less than 10^{-5} Torr. During the evaporation, the plates were held at the longest possible distance (~ 50 cm) from the evaporation source for ensuring uniform coating. The thickness of the SiO coating was $80\text{--}120$ Å as calculated from the evaporation geometry. The sample cells were prepared by pressing π -shaped Mylar spacers coated with thin unhardened epoxy between the two glass plates. After the epoxy setting, nematic Merck Phase V was injected through the spacer opening, and the cells were then sealed with epoxy. Two types of cells were prepared by mounting the glass plates with their respective in-plane projection of the direction of evaporation either parallel (p -type cells) or antiparallel (a -type cells). For the angles of evaporation used ($4^\circ\text{--}20^\circ$ with respect to the surface), the preferred anchoring direction is oblique in the plane determined by the direction of evaporation and the normal to the plate.^{11,18} Figures 1(a) and 1(b) show the director distribution respectively in the p and a type of cells before applying the voltage, as proposed by Guyon, Pieranski, and Boix¹¹ who have performed an optical study of the alignment in these type of cells (but for another nematic MBBA).

We verified that our a -type samples do not show a homeotropic alignment by simple polarizing microscope observations, nor a homogeneous (planar) orientation by measuring the conductivity of the samples in a magnetic field of 15 kG in parallel and perpendicular configurations and at zero magnetic field. The measurements were too rough to enable us to estimate the actual tilt angle.

The observations on the "sandwich" cells were done in the usual arrangement, with parallel light normally incident on the lower plate and microscopic observation from above.

The Merck phase V liquid crystal is a mixture of azoxy compounds:



and has a mesomorphic range between -5° to 75°C . The low frequency dielectric anisotropy is negative $\Delta\epsilon = \epsilon_{11} - \epsilon_{\perp} = -0.2$. The optical anisotropy $\Delta n = n_e - n_o = 0.29$. This data is given by the manufacturer. The dc conductivity anisotropy is positive (our measurements). The observations were made with an old and heavily used Reichert microscope. The magnification in the visual mode of observation was up to $200\times$. For photomicrography we used a motor driven model OM2 Olympus camera capable of taking up to four photographs per second. The photomicrographic magnification was up

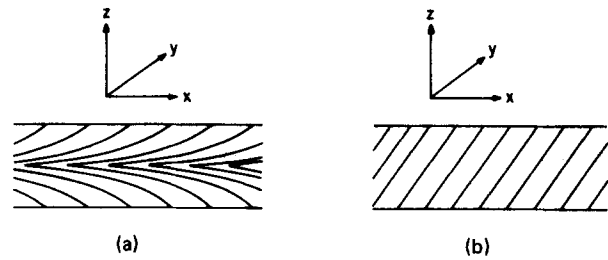


FIG. 1. (a) and (b). The alignment of the director at zero field in the p and a -type samples, respectively, that is assumed for purposes of discussion.

to $300\times$.

All the observations were at 20°C , if not otherwise specified.

III. RESULTS AND DISCUSSION

A. General

The three-dimensional instabilities encountered in the present study were found to focus the transmitted light into different $2D$ optical patterns at a few distinct focal planes. These distinct focal planes are easily resolved by the narrow field of view at microscope magnifications of $100\times$ and more. The existence of more than one focused image could probably have been anticipated on the basis of the observation by Penz that the $2D$ Williams domains focus different images of straight lines in different distinct focal planes.^{2,19}

The reason that some EHD in nematics can focus transmitted light, is that some nematic distortions associated with the instabilities can act as lenses converging or diverging incident light of special polarization. The nematics are birefringent and the refractive index of the extraordinary ray (n_e) is dependent on the angle between the direction of propagation of the light and the local optical axis (which is related to the director⁸). A distortion of the nematic for which the director has the proper functional dependence on the coordinates can thus create a gradually changing refractive index lens.

The light rays are deflected towards regions of higher refractive index. Since in the present case $n_e > n_o$, in our geometry, a ray polarized in a plane containing the director and the direction of propagation (i. e., an extraordinary ray) is deflected toward the region where the director makes a smaller angle with the plates. If, in this case, the director has the proper dependence on the coordinates, parallel extraordinary rays could be convergently focused by such a region. Parallel light can also be divergently focused by regions possessing an adequate gradual change to director directions more inclined to the plates. The reason some of the associated distortions of the encountered instabilities have the right functional dependence for focusing light is probably because, under the most commonly used boundary conditions, the equations for static equilibrium under torques and the hydrodynamic equations in nematics tend to have simple harmonic solutions for the dependence of the director direction on coordinates

(which were shown by Penz¹⁹ to cause the extraordinary rays to focus). However, we think that some other light focusing distributions encountered during this work are not of a harmonic type. The regions of distortion in the nematics not having the proper director distribution for focusing will tend to diffuse the incident extraordinary rays.

The ac low-frequency conductivity of our samples is of the order of 10^{-11} mho cm^{-1} .

The measured dc resistance of our samples is dependent on the history of the voltages previously applied to them and could vary in a range of 1–2 orders of magnitude. The overall resistance of a 50 μm thick sample of 3 cm^2 area for example will typically increase from 10^8 to 10^9 Ω in an hour when applying 1 V on the plates and then become 2×10^7 Ω when the polarity is suddenly reversed (probably due to reversible electrode polarization). The thresholds for the various events to be described in this paper also change in relation to the previously applied voltages, probably for the same reasons for which the resistance of the samples changes. Because of this, the voltages at which various events are noted in this work should be taken as typical only. The results of actual experiments could differ by up to ~15% from the given values. Many of the patterns described below appear sometimes as transitory. This is most probably related to the increase in resistance of the sample when it is kept at a dc voltage which causes the increase of the threshold voltages. However all of these patterns can be made to last for many hours by properly adjusting the voltage, and by no means are they of a transitory nature.

The following notation will be used below:

PIDAP—Projection of the initial director alignment on the plane of the plates; P—Polarizer; A—Analyzer; pll and ppd—Parallel and perpendicular to PIDAP respectively. Thus, for example, pll P, ppd A means a configuration with crossed polars in which the polarizer is parallel to PIDAP.

The photographs presented have their vertical direction parallel to PIDAP [\times direction of Figs. 1(a) and 1(b)], except photograph 2 Plate 7 for which the PIDAP is rotated 45° clockwise.

B. Direct-current instabilities

1. *p*-type Cells

a. Low voltage instabilities. Photographs 1 through 4 of Plate 1 show the image patterns of the dc instability in a 50 μm thick *p*-type cell taken at increasing distance between the objective and the sample (pll P, pll A). The patterns of photographs 1 and 2 are divergently focused, while those of 3 and 4 are convergent. The SiO evaporation angle was 4°. The applied voltage was 8 V. Similar patterns are found in cells 25–100 μm thick.

The closed, rounded curves of photograph 3 are seen out of focus in photograph 2. The straight lines of pho-

tograph 4 connect the centers of the neighboring hexagons, except in the PIDAP direction. Photograph 5 Plate 1 is taken with pll P and ppd A at the same focal plane as photograph 2 and clearly shows a V-shaped figure at the center of each hexagon. A similar image is formed with a ppd P, pll A configuration of polars, but the V-shaped bright figure in the middle of the hexagon is shorter and sharper. In the ppd P, ppd A configuration the pattern is changed with respect to photograph 5 by having the bright parts become dark and vice versa. These optical observations show that the V shapes are the image of a distortion in which the director is no longer in the xz plane [Fig. 1(a)], characteristic to other instabilities in geometries with oblique alignment at the walls in nematics possessing a negative viscosity coefficient α_3 .¹² The direction of the V shape does not change when the polarity of the electrodes is changed, and the vortex of the V shape is pointing in the increasing x direction of Fig. 1(a).

The period (the distance between the hexagon centers) is about 100 μm which is twice the sample thickness, as expected for such a dc EHD.

In all, photographs 1–5 Plate 1 disclose what we believe to be a flow pattern.^{20(a)} Photograph 2 Plate 1 broadly resembles the visualization of the hexagonal flow pattern of the Benard instability,^{20(b)} but features showing departure from hexagonal symmetry are clearly displayed in the patterns shown in photographs 3, 4, and 5.

The threshold voltage for the hexagonal pattern (which was not accurately measured because of the above-mentioned dependence on the previous applied voltages) does not seem to depend on the sample thickness in the 25–100 μm region.

The hexagonal patterns are generally moving as a whole in the x direction [Fig. 1(a)], at typical speeds of 10–100 $\mu\text{m}/\text{min}$. In the limited time we spent studying this motion, we could not find a clear relation between the magnitude and sign of the velocity of this movement and the applied voltage, except for the observation that immediately above the voltage at which the hexagons first appear, the velocity is increased by increasing the voltage.

As photograph 1 Plate 2 shows, the hexagons sometimes coexist with stripes, which are not the classical Williams domains since they tend to form in a direction which is almost perpendicular to the direction expected for the Williams domains. [Similarly oriented stripe patterns have been encountered before in the geometry of Fig. 1(b), Ref. 12(b)]. For reasons as yet unknown, these stripes appear only in some of our samples. In this kind of samples the stripes usually form at a lower voltage than the hexagons (1–2 V lower), and they transform into hexagons when the voltage is increased.

Photograph 6 Plate 1 shows the deformation of the pattern of photograph 4 Plate 1 at a voltage of 11.5 V, far from the threshold but not yet in the turbulent regime. Photographs 3 and 4 Plate 2 show typical occurrences at still higher voltages (typically 12–14 V). The hexagonal

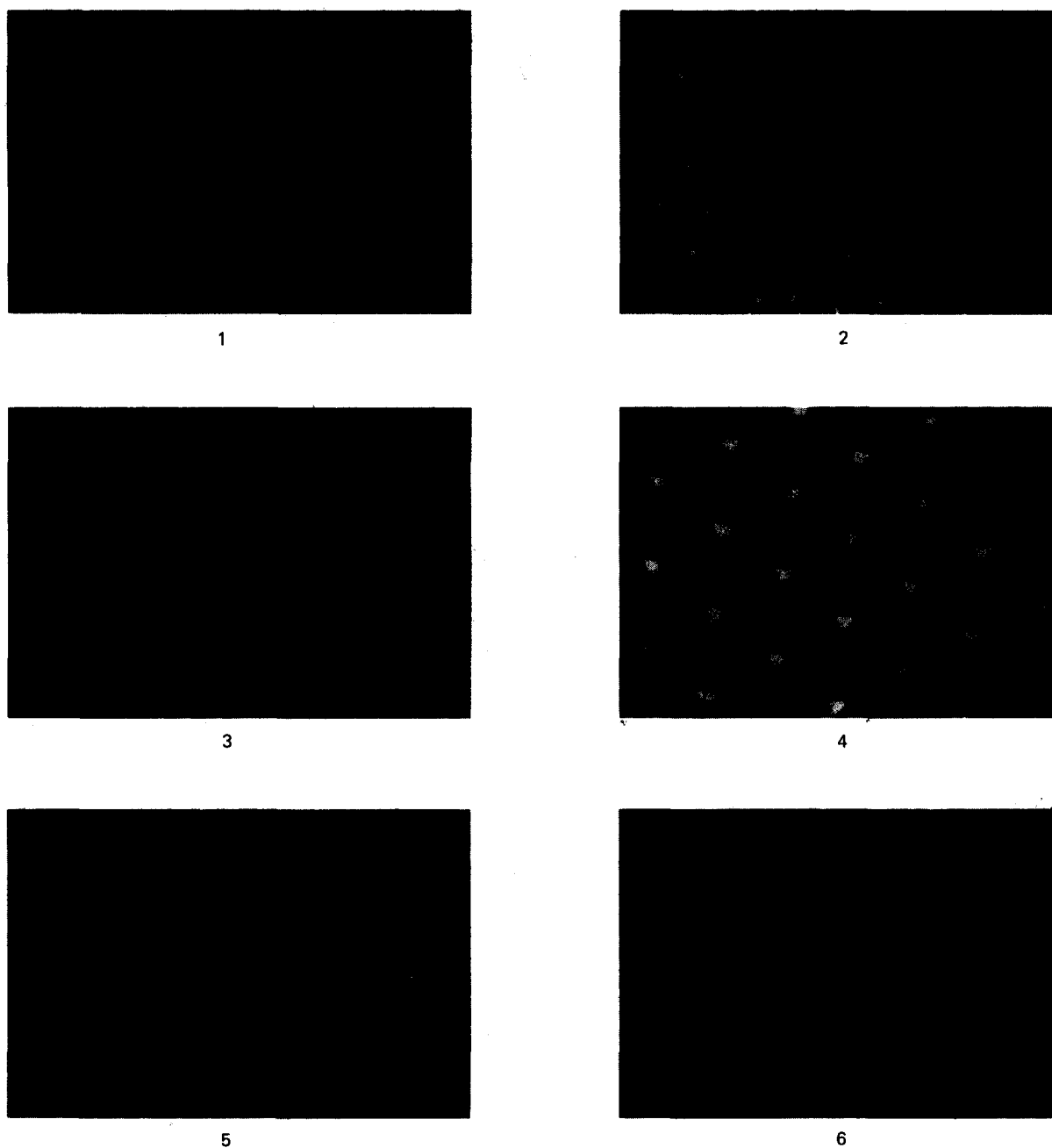


PLATE 1. Low voltage dc instability in $50\ \mu\text{m}$ p -type cell [cf. Fig. 1(a)]. The photos show regions of $0.6\ \text{mm}$ horizontal dimension. Photos 1-4 and 6 are taken at $8\ \text{V}$ with pll P, pll A. Photos 1-4 show the sequence of patterns occurring at different focal planes as the microscope objective is raised. (Photos 1, 2 are divergently focused patterns; Photos 3, 4, and 6 are convergently focused patterns.) Photo 6 shows the change in the pattern of photo 4 when the voltage is increased to $11.5\ \text{V}$. Photo 5 is taken with pll P, ppd A. The patterns are moving in the vertical direction of the photographs with a velocity of the order of $100\ \mu\text{m}/\text{min}$.

grid distorts and less regular flow of the individual hexagons occurs. Two or more hexagonal flow cells will sometimes coalesce to form a new hexagon, which later decreases in size; also new hexagons and other polygons appear in the free space created by the motions of the hexagons. Some hexagons divide into two.

b. Higher voltage instabilities (p -type cells). At higher voltages, typically 14 - $17\ \text{V}$, the hexagonal patterns were observed to break down into smaller, chaotic flows of a few μm dimensions. Photograph 5 Plate 2 is taken just before such a process starts occurring

after a sudden increase of voltage from 11 to $16\ \text{V}$. At still higher voltages, typically over $17\ \text{V}$, surprisingly enough, after a period of waiting of a few minutes, large areas of the samples become organized into two kinds of stripes oriented at small angles with the x direction. These two types of stripes occur more extensively in the a -type samples at similar voltages, and will be described below in relation to the dc instabilities in the a -type cells.

The typical voltages at which all the above phenomena occur is lowered when the temperature increases.

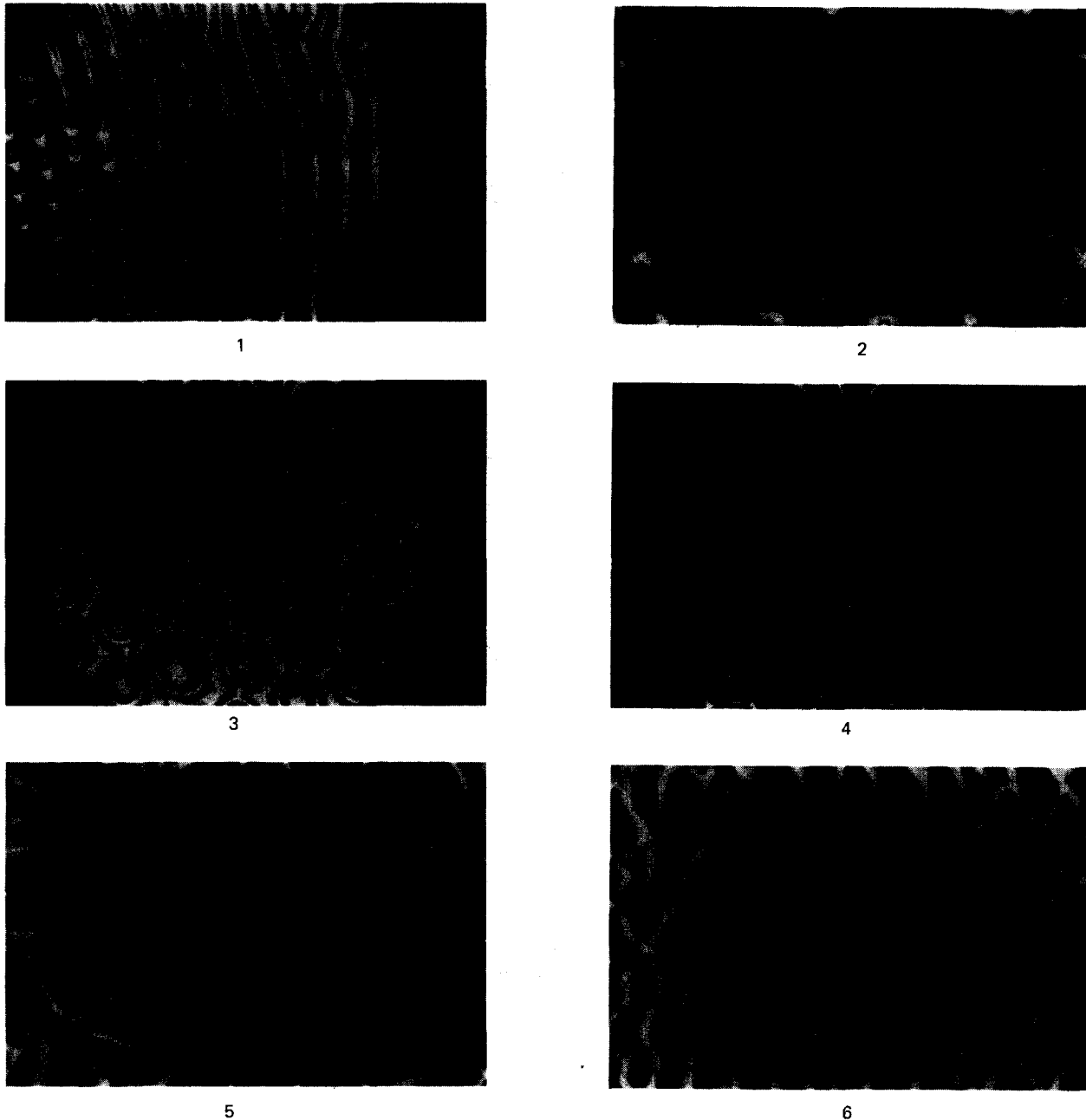


PLATE 2. Photos 1–5 show low voltage dc instabilities in p -type cells. Photo 1 shows coexistence of hexagons with longitudinal (x direction aligned) stripes. Photo 2 shows a convergently focused hexagonal pattern (aged p -type sample). Photos 3 and 4 are of a $50\ \mu\text{m}$ p -type sample at 12 V dc. A process in which cells of the low voltage p -type instability unite, divide, diminish or grow in size, or move into voids occurs at higher voltages (12–14 V) with a characteristic time ~ 60 s. Photo 5 shows a hexagonal pattern on the way to disorder when the voltage is suddenly increased from 11 to 16 V. Shortly after this photograph was taken, the pattern broke down into smaller size, chaotic flows. Photo 6 shows an ac conduction instability in an $50\ \mu\text{m}$ a -type sample 3.7 V dc.

c. Effects of aging on the p samples. The following effects of aging have been noted in a period of 1–4 months in our samples. Some of the effects of aging could be reversed in some samples by applying 200–300 V for about an hour.

At first the hexagons start becoming irregular polygons (4–7 sides) the average number of sides decreasing in time down to four. A light diverging pattern of rhombi that are almost squares (“chicken grid”), with diagonals in the x and y directions (that are not visible)

is seen in old samples. This pattern is associated with a converging circular shape pattern (similar to the one in photograph 3 Plate 1) showing up in a higher focal plane, and a converging pattern that is sometimes hexagonal at a still higher focal plane (photograph 2, Plate 2; the reason the hexagonal pattern appears broken in this photograph is interference caused by use of too small an aperture of the field diaphragm of the microscope.) Another effect of aging of the samples is that the contrast between bright and dark areas of the figures decreases.

2. *a*-type Cells

a. Low voltage instabilities. A typical sequence of events which actually occurred in a 50 μm thick *a*-type cell as the voltage was gradually increased from zero is described below. The SiO evaporation angle was 4° . We again remind the reader that the voltages associated with these events should be taken only as representative for reasons given above.

At 3.7 V an irregular polygonal pattern starts forming (photograph 6 Plate 2). This pattern is weakly seen, and we could not relate it to the other patterns described below. It also persists at low frequencies (≈ 10 Hz) while the instabilities described below in this paragraph are dc regime.

At ~ 7.5 V flows start nucleating at distortion sites of the nematic. (The observation showing that these are flows is discussed in Sec. IIIB 4). These distortions are generally related to irregularities in the SiO coating. Extensive nucleation of flows, that are associated with pronglike distortions, occurs at the side walls of (cf. photograph 1 Plate 7, right). Air bubble boundaries distortions and inversion walls in the nematic could also be regions of nucleation. As the voltage is increased, each flow extends in size. A process of nucleation and growth is shown in photographs 1–3 Plate 3 (but for a higher excitation voltage).

The flows and associated nematic distortions represented in photograph 3 Plate 3 will be called “flow figures” below. The two protrusions at the bottom of the flow figure pointing down and to the side in the same photograph will be called branches. Anticipating a more detailed description, the part delimited by the bright rounded closed curve in the upper middle part of the flow figure (same photograph) is observed to contain a toroidal flow which will be called “core flow”.

At 8.3 V the flows start detaching themselves from the original distortion site at coating defects and begin moving (as shown in photograph 4 Plate 3 for a higher excitation voltage). The movement is in the positive x direction of Fig. 1(b) when the *upper plate* is the positive electrode. After traveling ~ 100 μm without too much visible change of shape, the flow figures become of weak contrast, slow down and disappear. As the voltage is increased, the distance traveled by the flow figures before disappearing increases. The velocity of the movement in the x direction increases with the voltage. (A typical velocity is 100 $\mu\text{m}/\text{min}$.)

At 10 V the flow figures seem to travel any distance permitted by the sample length. A host of such solitary (nondispersive, i. e., not changing shape) flow figures is seen in the left side of photograph 1 Plate 7.

We also observed on some occasions what appear to be flow figures without core flows (the branches unite at the place where the core flow occurs in the flow figure). These objects were formed at the same range of voltages; some were static and others (created at coating defects sites) moved a distance which increased with voltage, like the flow figures. No regime of solitary propagation (see above) was observed; an increase of

voltage led to the creation of core flows before this could possibly happen. We hope to describe these objects elsewhere in more detail.

As the voltage is further increased to 11.5 V, the flow figures start a replication process. This is described below.

Plates 3 and 4 show the growth of a flow figure at a surface defect site, the subsequent movement of the flow figure [upward in the photographs as well as along the x direction of Fig. 1(b)] and the replication process, when a voltage of 11.5 V has been applied to a 50 μm thick sample. The polars were in the pll P, pll A configuration. The photographs were taken at 10–60 s intervals. As these photographs show, the newly generated flow figures start forming on the two bright branches. The branches are converging the light polarized in the x direction meaning that they have a heap-like structure, the director slope relative to the plates changing sign at the place of maximum luminosity. The director remains in the xz plane in the region of the branches. Notice in photograph 5 Plate 3 the formation of the daughter flow figure on the right branch of the older moving flow, also the growth of a new flow figure at the place of the defect in the SiO coating. In photograph 6 same plate, another group of moving flow figures enters the frame of the picture in the lower left corner.

The replication process leads to the creation of a moving grid of flow figures (typical velocity 250 $\mu\text{m}/\text{min}$ in a 75 μm sample), the distance between two next-neighbor core flows being approximately twice the sample thickness. Photographs 3–6 Plate 7 show four image patterns of this grid (when it is fully formed) at four different focal planes, as the objective is moved further from the sample (pll P, pll A). The points of photograph 3 are located at the intersection of lines connecting the centers of the core flows of photograph 5 horizontally and vertically. The direction of motion of the grid is downwards in these pictures. These patterns are seen with slight changes in detail in unpolarized light. No systematic threshold dependence on sample width have been observed for all the above phenomena in the range 25–100 μm . However there seems to be a tendency to fast movement of the grids in the thinner samples.

Plates 5 and 6 show the process of replication at a higher excitation voltage (13 V). These photographs show that the new core flows are created when part of older core flows open a longitudinal “cut” in one of the two branches and leak through to form new core flows (as best seen in photographs 3, 4, 5, Plate 5). No such process was observed visually at lower voltages close to the threshold for replication, and our photographic equipment and skills were not good enough to make decisive observations on the question of whether or not the same mechanism occurs close to the threshold. Thus, at the lower voltages the new core flows appear so far to be created by a local process at the proper distance from the older core flow (cf. photograph 5 Plate 3), although the possibility of the “leak of flow” process which happens at higher voltages is not yet

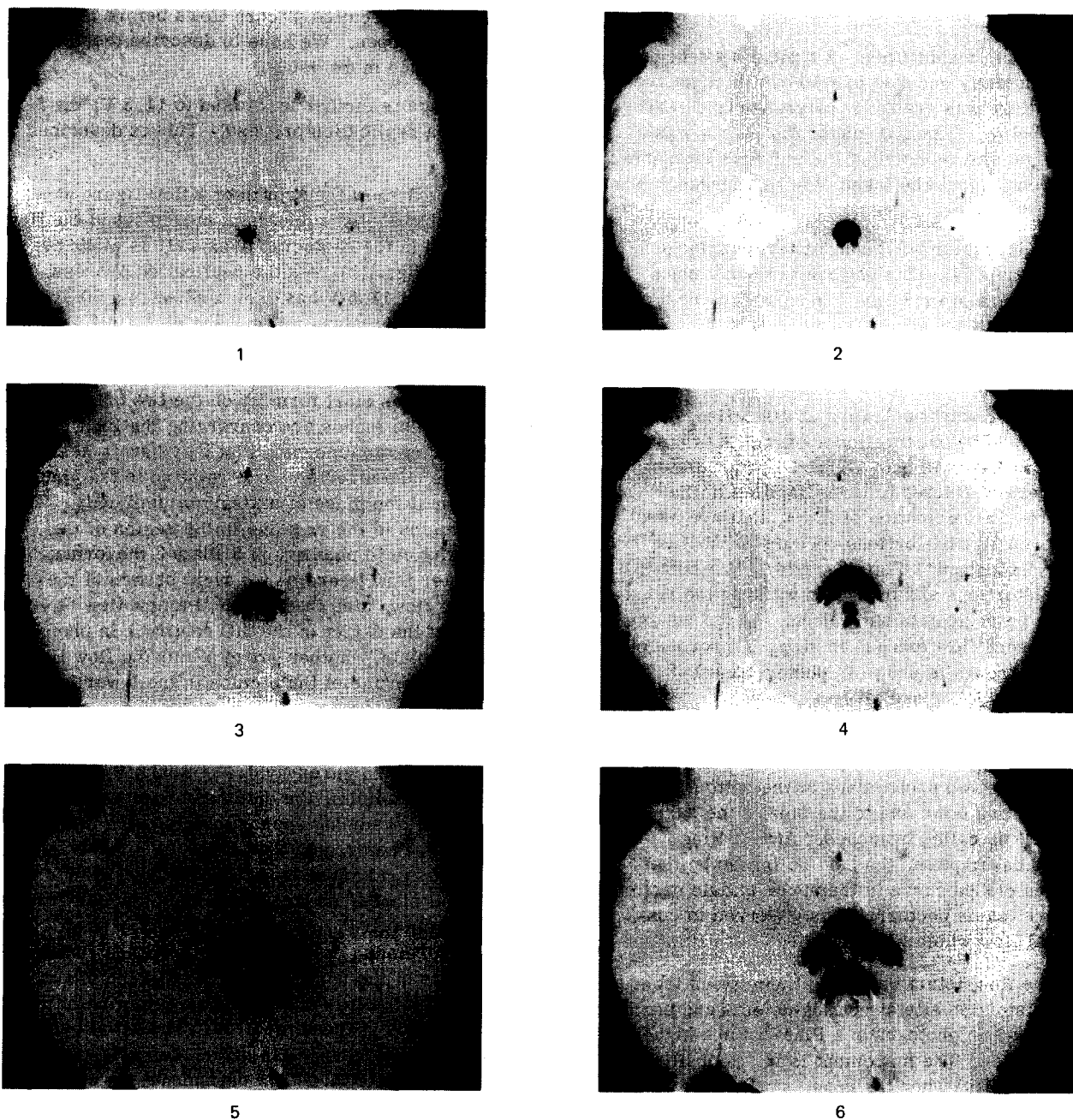


PLATE 3. The growth of an α -type low voltage dc instability after a voltage of 11.5 V dc is applied ($50 \mu\text{m}$ sample) [cf. Fig. 1(b)]. The photos show a region 1.1 mm across and are taken with pll P, pll A at 10–60 s intervals. Photos 1–2 show a flow figure growing at a distortion site associated with a defect in the SiO coating. Photo 3 shows the flow figure detaching itself from the defect site and starting to move in the PIDAP direction (velocity $\sim 3 \mu\text{m/s}$). Photo 4 shows a new flow figure forming at the place of the defect, while the first flow has moved away. The two “branches” attached to the first flow and oriented aside and backwards had increased in size too. Photo 5 shows a “daughter” flow that has appeared on the right branch of the first flow; a second daughter is shortly to be formed on the brighter spot of the left branch. Photo 6 shows the first flow figure created as well as the two flow figures replicated from it, which now have moved up, while the second flow figure created at the defect site has detached itself from this site and has also moved up. A group of moving flow figures created elsewhere is now seen in the frame in the left lower corner.

totally excluded. In some “bad” samples in which the grid of flow figures that is formed is quite irregular, the branches of some flow figures have a permanent region of flow along and inside the branch (cf. photograph 1 Plate 8). The quality of the sample is probably related to the quality of the SiO coating and is not sensitive to a slight degree of misalignment between the plates.

The horizontal diffuse bright lines, some of which seem to be extending from the branches in Plates 5 and especially in Plate 6, connect the group of flow figures with another similar group moving parallel to it at the left, outside the frame of the photograph. These lines seem to represent a mode of a similar nature as the branches and appear to be induced by the branches as they form during the replication. Like the branches,

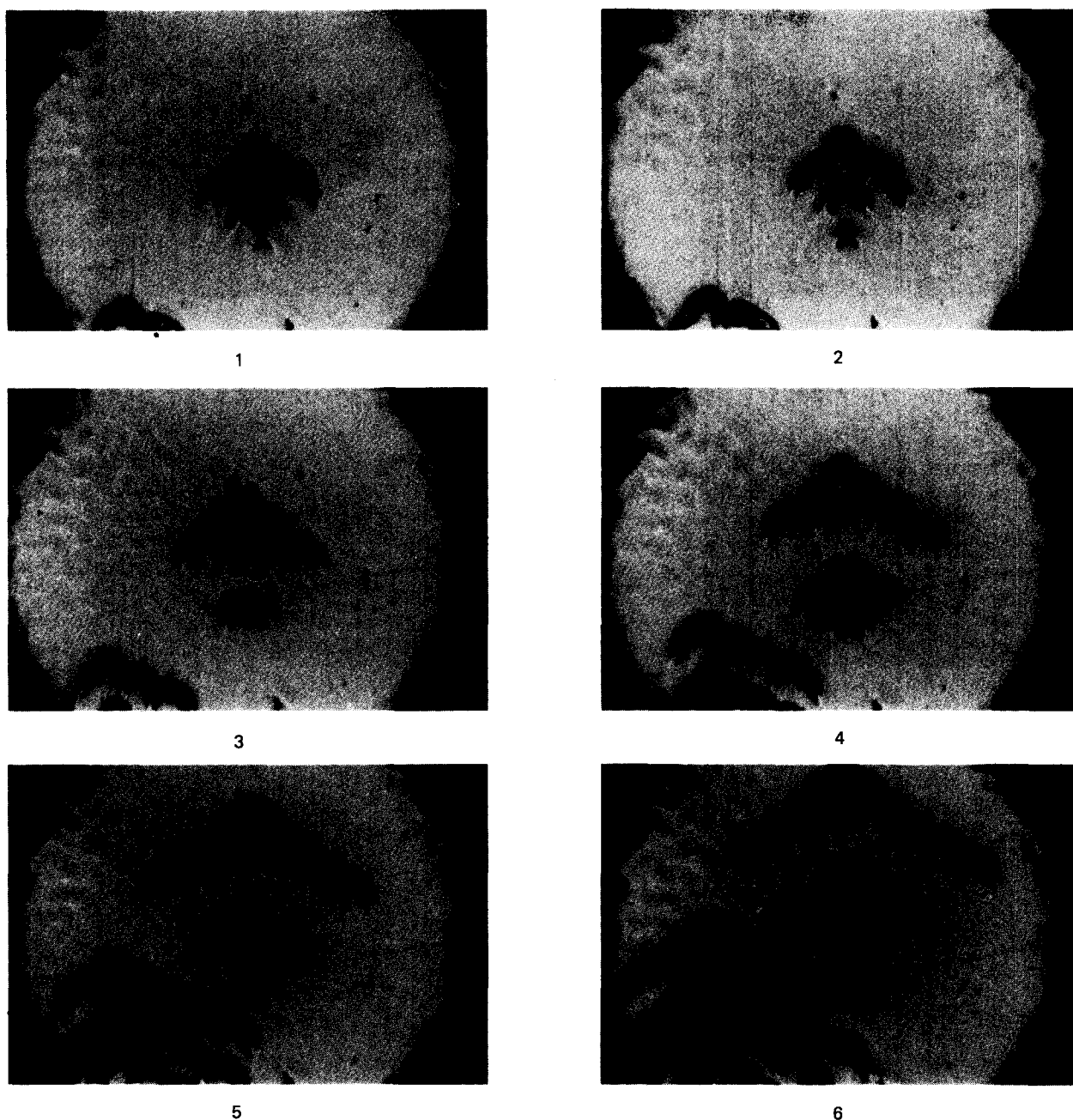


PLATE 4. Photos 1–6 show further stages in the development of the instability of Plate 3 involving new flow figure formations at the coating defect site, flow figure movement and replication.

these are causing the extraordinary rays to converge and are probably (broader) splay-bend walls over which the tilt of the director in the xz plane changes direction.

At higher voltages (≥ 13 V) lines similar to these, of long extent in the y direction [Fig. 1(b)] but sharper and brighter and not so regularly spaced seem to appear even before the flow figures appear, immediately after the voltage is turned on. The flow figures seem to nucleate on these lines shortly *after*. Better photographic abilities and equipment could help clarify this matter. The flow figures are at first dispersed, in this case quite irregularly on these lines, and the periodic grid then organizes itself in a few minutes afterwards. The way in which the grid becomes regular is

by xy plane movement of the core flows and by combination and division of individual flow figures.

At about 2 V above the voltage at which the grid of flows first appears, two colored (blue for pll P, pll A) “wakes” follow the flows in their movement along the x direction. These “wakes” are seen with pld P also, which is an indication that the director gets locally out of the xz plane. For this kind of sample thickness, the relatively pure colors indicate that in the “wakes” the director is more tilted, i. e., closer to the perpendicular to the plate planes. The “wakes” follow the two crescentlike figures described below. When the stage is turned 45° , these wakes show up to be striped across. This shows the existence of director orientation waves.

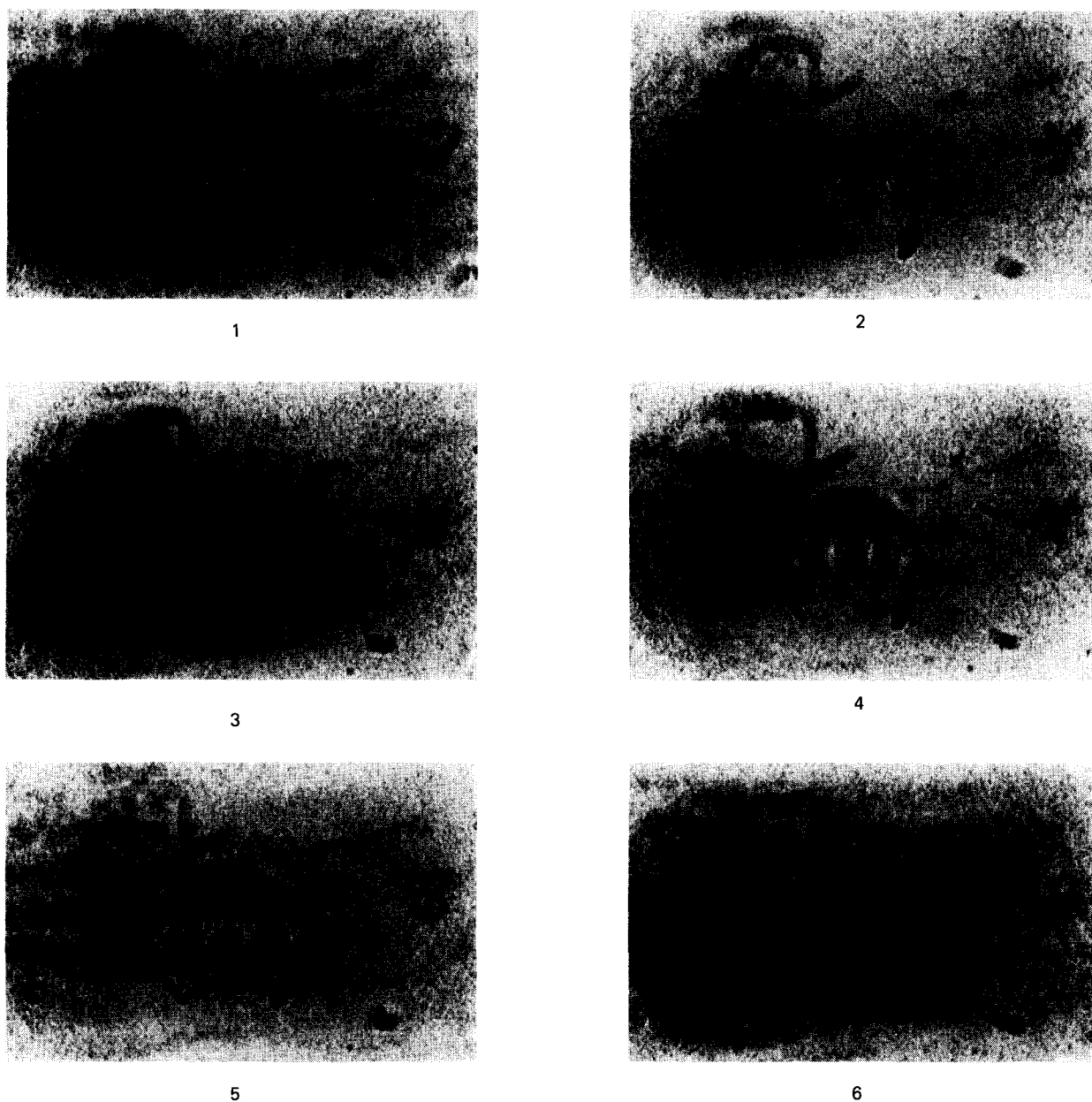


PLATE 5. Shows the growth of the a -type low voltage dc instability at a higher excitation voltage (13 V). The photographs are taken at 1 s intervals. The first flow figure (photo 1 Plate 5) grows at a distortion site associated with a defect in the SiO coating. As seen in photo 3, in the process of replication under this voltage, part of the older flow "leaks" through a longitudinal split in a branch to form a new flow center ("core flow").

(The director alternately lies within and out of the xz plane.) Photograph 2 Plate 7 is taken at a still higher voltage (14 V), with PIDAP rotated 45° clockwise to the crossed polars. (The polarizer orientation is in the vertical direction of the picture.) This photograph shows the striped structures of the wakes. (At this higher voltage the two wakes are united across into a single one, and the grid is a little distorted.)

A striking feature of the instability, which was too difficult for us to photograph, is an interference-like pattern which appears in each of the core flows. When the microscope is focused inside the nematic, close to the upper plate, bright-dark alternate concentric circles are seen (no extinction cross under crossed polars).

As the objective is lowered toward the bottom plate, the circles decrease in diameter and number and shrink to a common center, after which, when still lowering the objective, the interference-like figure shown in Fig. 2 grows in size, to disappear out of focus approximately when the objective focal plane reaches the bottom of the nematic. The level at which the circles shrink to a point is at about the middle plane of the sample. When the sample is turned over, the concentric circles are still visible in the (new) upper half part and the other figures in the lower half. The figure of concentric circles is seen also without polarizer and analyzer. It is very probable that the figure seen in the lower half of the sample is as seen in Fig. 2, because of the optical distortion created by the nematic director distribution in

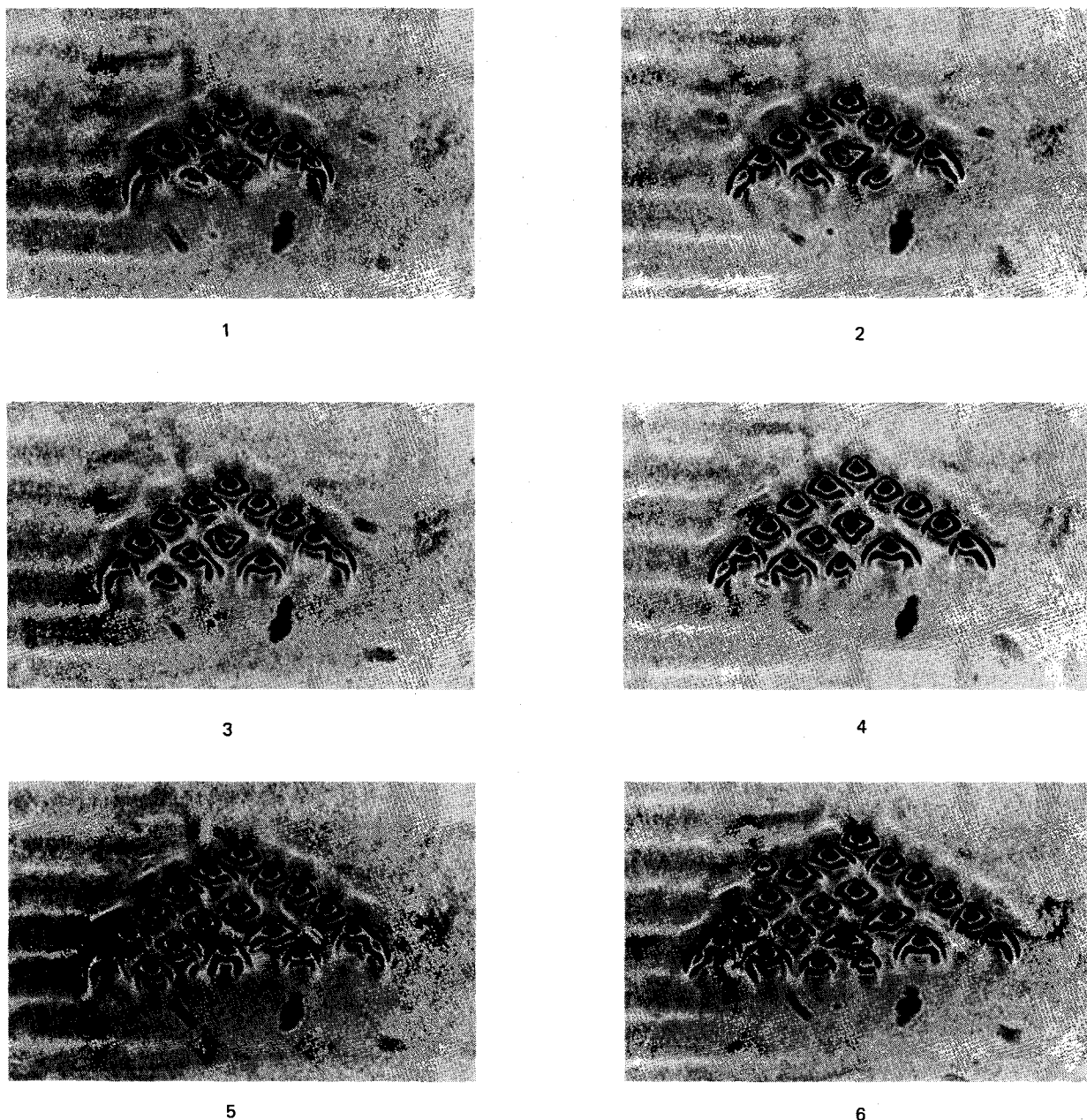


PLATE 6. Continuation of the process shown in Plate 5.

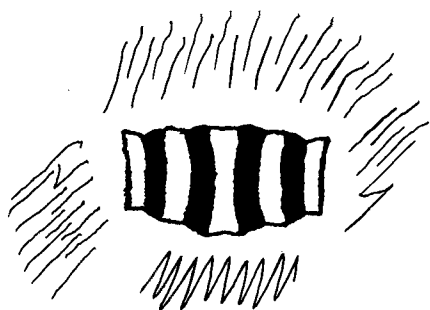
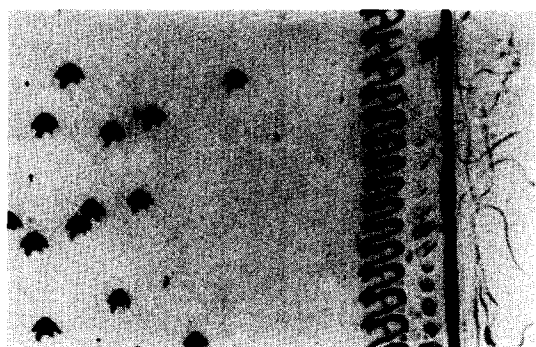


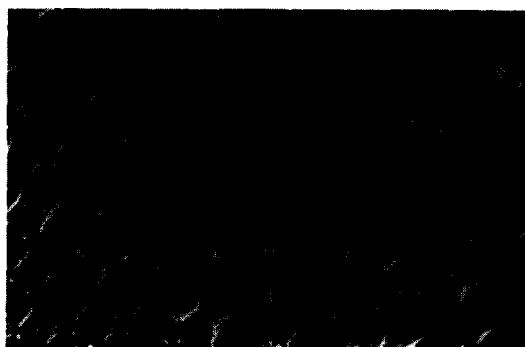
FIG. 2. Interference figure seen in the central part (core flow) of the flow figures of the low voltage *a*-type instability (photo 5 Plate 7) when the microscope is focused on a plane in the lower part of the sample. The vertical direction in this figure corresponds to the *x* direction in Fig. 1(b).

the upper half of the samples. At about 2 V above the "threshold" for replication, the concentric circles are embraced laterally by two crescentlike figures of optical properties similar to the V figures of the hexagonal pattern. These optical properties show director orientation out of the *xz* plane. Further work is required to ascertain whether any artifacts are contributing to Fig. 2.

b. Higher voltage instabilities (a-type cells). As the voltage is increased to 15–16 V, the flows of the grid start dividing and uniting like in the case of the hexagons. All the movements bringing flows together or apart occur on the branches. At about 16–17 V the branches bend back more and more towards the *x* di-



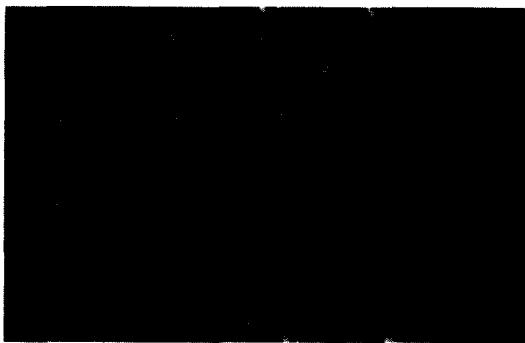
1



2



3



4



5



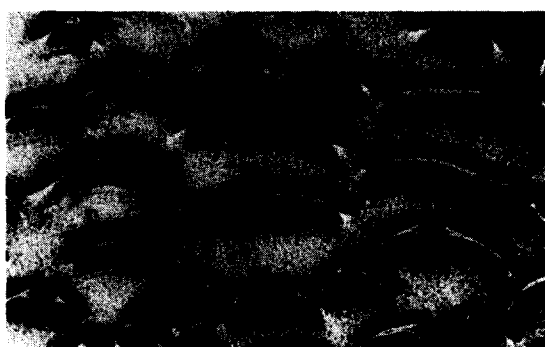
6

PLATE 7. The α -type low voltage dc instabilities in a $90 \mu\text{m}$ sample. Photo 1 is taken at 10 V (below the voltage necessary for replication). A host of solitary flows can be seen at the left. At the right of the photo deformations appear which are associated with flow nucleations at the wall (seen as the longitudinal dark line). Photo 2 shows the grid of flows of the instability at 14 V with the sample at an angle of 45° , between crossed polarizers. The striated wakes, which are seen to follow each flow figure, are regions where there is a (moving) periodic distortion in which the director alternately lies within and out of the xz plane [cf. Fig. 1(b)]. Photos 3–6 show image patterns of the grid of flows at four focal planes as the objective is raised (12 V on a $90 \mu\text{m}$ sample). The photographs show a region $\sim 1.1 \text{ mm}$ across. The grid moves downwards.

rection, and the flow becomes more and more chaotic (photograph 2 Plate 8). After a period of waiting of tens of seconds to minutes, large regions of the sample (typically over 30% of the area at 20–30 V and usually more at higher voltages) reorganize into two kinds of striped patterns and their variations, while the other regions remain turbulent. The turbulent regime, before the appearance of the stripes, might indicate that some process such as the suggested reversible polarization which increases the resistance of the sample (cf. Sec. IIIA) must take place before the striped in-

stability can occur. The striped patterns appear on the p type of samples too, although to a lesser extent, with shorter stripes, and more defects.

The first kind of stripes have a width comparable to the sample thickness when they first appear at about 18 V, but they decrease in width approximately as E^{-1} . We have seen relatively pure modes of these stripes up to $E = 80 \text{ kV/cm}$ at which point they have a curly aspect if the field is applied suddenly. At higher fields the stripes appear weakly on a multicolored mosaic



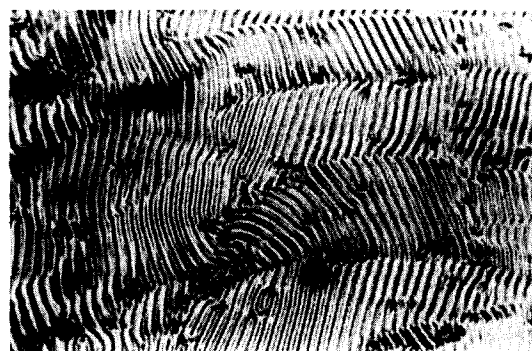
1



2



3



4



5



6

PLATE 8. Photo 1 shows an irregular grid of an α -type low voltage dc instability in a "bad" sample. Photo 2 shows deformation of the α -type low voltage dc grid of flows at higher voltages (~ 16 V). Photos 3 and 4 show a variant of the variable grid mode pattern. The two photographs were taken at the same position at an interval of two seconds and show a movement of the fronts between the regions of stripes of different orientation. Photos 5 and 6 show a region of a variable grid mode pattern at 17.5 V (photo 5) and after a sudden increase from this voltage to 35 V when the alternate skew-straight pattern is formed (photo 6).

textured background and probably disappear at about 120 kV/cm. Sometimes the stripes are associated with colors. We do not know yet whether this is a dc or an ac conduction regime EHD.

At low voltages (18–25 V) the texture of the stripes is formed by groups of stripes oriented at \pm a small angle α with the PIDAP ($\alpha \sim 20^\circ$ – 25°). Sometimes the separation fronts between regions of stripes with α of different sign are moving. Photographs 3 and 4 Plate 8 which show this kind of movement were taken at the same position at an interval of about 2 s.

The E^{-1} wavelength dependence and the colors appear

to indicate that this striped pattern is related to the variable grid mode as described by Greubel and Wolff.^{15(a)} The difference is that the present grid has the orientation of the stripes at small angles α with PIDAP, while the pattern described by these authors is oriented perpendicular to the initial director orientation. Another similarity with the variable grid mode as described by Greubel and Wolff is that dust particle movement can be observed in the sample. Pure flexoelectric instabilities as described in Refs. 13(b), are not expected to exhibit this kind of movement and are reported as not showing this in practice.¹⁴ The present instability could be related to the "E.D." instability of Ref. 12(b),

classified in Ref. 15(b) as variable grid mode. [However the present instability does not seem to exhibit the periodic changes of the angle of the director with the zx plane as does the dc EHD of Ref. 12(b)]. Although the relation to the variable grid mode of Ref. 15(a) might be only superficial, we shall call it for convenience, a "variable grid mode variant" (VGMV).

The following observations on the colors and the dust particle movement in this pattern as they appear in our a -type samples are consistent with the Carr model described in Sec. I, and with related experiments (cf. Refs. 16). Dust particles are seen to be moving somewhat slowly when they are between the bright lines which outline each stripe, but they are seen to be thrown violently into motion (most of the time) when they hit a bright line. This can indicate that the distortion walls corresponding to the bright lines are regions of very strong flows in the direction of the perpendicular to the plates, unless the large momentum transfer to the particle is due to electrostatic forces. When dust particles are in the region between these walls they are seen rotating around an axis parallel to the walls and much faster than in any other situation observed by us, which can be another indication that this is a region of strong velocity gradients caused by strong flow of opposite direction in alternate walls.

When the sample is observed between polarizers, the colors of the stripes can be quite pure, which for the present kind of sample thickness indicates that the director is aligned close to the perpendicular to the plates. (This is of course against the tendency of the field which acts to align the molecules parallel to the plates in this negative dielectric anisotropy nematic.) For strong flow in the walls causing strong shear, one expects uniform director alignment between the walls. This is actually seen in our samples, since each stripe is colored uniformly across in the region between neighboring bright lines, which indicates uniform alignment. Furthermore, in some occasions, like in $50\ \mu\text{m}$ a -type samples at 50 V every other stripe has the same color (e.g., the colors alternate from stripe to stripe between bluish and brownish hues). This is again consistent with the assumption of the shear flow alignment. The main contribution to the torque on the director that induces alignment in our samples is caused by the flow in the walls. This component is proportional to dv_z/dx (cf. Fig. 1) which alternates in sign in alternate stripes. The component dz_z/dx is nonzero because of the small angle α between the stripes and the x direction. Since the boundary conditions are oblique, equal but opposite torques in the neighboring stripes will induce different angles of alignment in alternate stripes, thus also alternate colors.

When the voltage is suddenly increased from ~ 17 V to 30–40 V, one observes in large portions of the VGMV that every other line bends itself into a static skewed-shape (relaxation time ~ 2 –3 s). This is a reversible process. The skew bending of the focal line corresponds of course to a skew bending in the xy plane of the (probably splay-bend) deformation (or wall). Photograph 5 plate 8 shows the pattern at 17.5 V in a 75

μm sample, while photograph 6 of the same plate shows the same region of the sample after a sudden increase in the voltage to 35 V. It is remarked that the zigzags form such that substantial portions take on the angle α opposite in sign to that of the initial orientation of the lines. Photograph 4 Plate 12 shows a region of alternate straight-skewed lines where bright spikes are seen to form at some of the zigzag vortices. Increase of the voltage to 50 V causes the skewed lines to break and curl at these sites in some of the samples.

At the dividing fronts (moving or static) between stripes of different sign of α , the skewed lines become straight and vice versa.

The skewing of some of the lines (walls) to form the alternate skewed-straight pattern is only one example of a more general occurrence of skew bending in the variable grid mode variant, which will be illustrated below by photographs and will be called "folding" from now on. By increasing the voltage on the sample at various rates from one value to another, many forms of the VGMV which show folding can be obtained. If, for example, the voltage is suddenly increased from about 11 V to about 100 V in an a -type sample, a pattern in which the folding mimics the low voltage a -type dc instability unit cell boundaries is obtained (rise time ~ 1 s). This is illustrated by photographs 1 and 2 plate 13, the first showing the low voltage a -type dc instability at 11.3 V, the second being taken 2 s after a sudden increase of the voltage to 111.3 V ($90\ \mu\text{m}$ sample). Obviously, this folding, like the folding of every alternate line, which leads to the formation of the alternate skew-straight pattern, is the way the instability increases its wave number k to adjust to the $\sim E^{-1}$ dependence of λ from the given starting condition. Conversely the mechanism of decreasing k when lowering the voltage at a moderate rate (~ 10 V/s) from a high voltage grid is an unskew bending (unfolding). If this unfolding is pursued to the voltage values where the low voltage a -type dc instability exist (~ 11 V), it appears that the closed bright curve, which delimits the core flow of each flow figure in photograph 5 Plate 7, is created smoothly out of a bright line of the VGMV. This indicates a topological and rheological likeness of the two deformations. Photographs 3 and 4 Plate 13 show two steps in the unfolding of pattern 2 Plate 13 (voltage decrease $dv/dt \sim 10$ V/s). Specifically photograph 4 shows a stage close to the reformation of the low voltage a -type dc instability. Photograph 6 Plate 13 shows the folding pattern formed from the starting 35 V, $90\ \mu\text{m}$ a -type sample pattern shown in photograph 5 plate 13, after the voltage was suddenly increased by 100 V. Photographs 7 and 8 show two stages in the unfolding of the pattern of photograph 6 same plate. Note "approximate reversibility" as seen by comparing photographs 5 and 8.

The second kind of striped pattern that we observed is associated with inversion walls. The stripes form in large areas of the sample which are separated from the other parts of the nematic by surface disclination lines. The stripes are close to being parallel to the PIDAP but rarely are really parallel, and then only for short

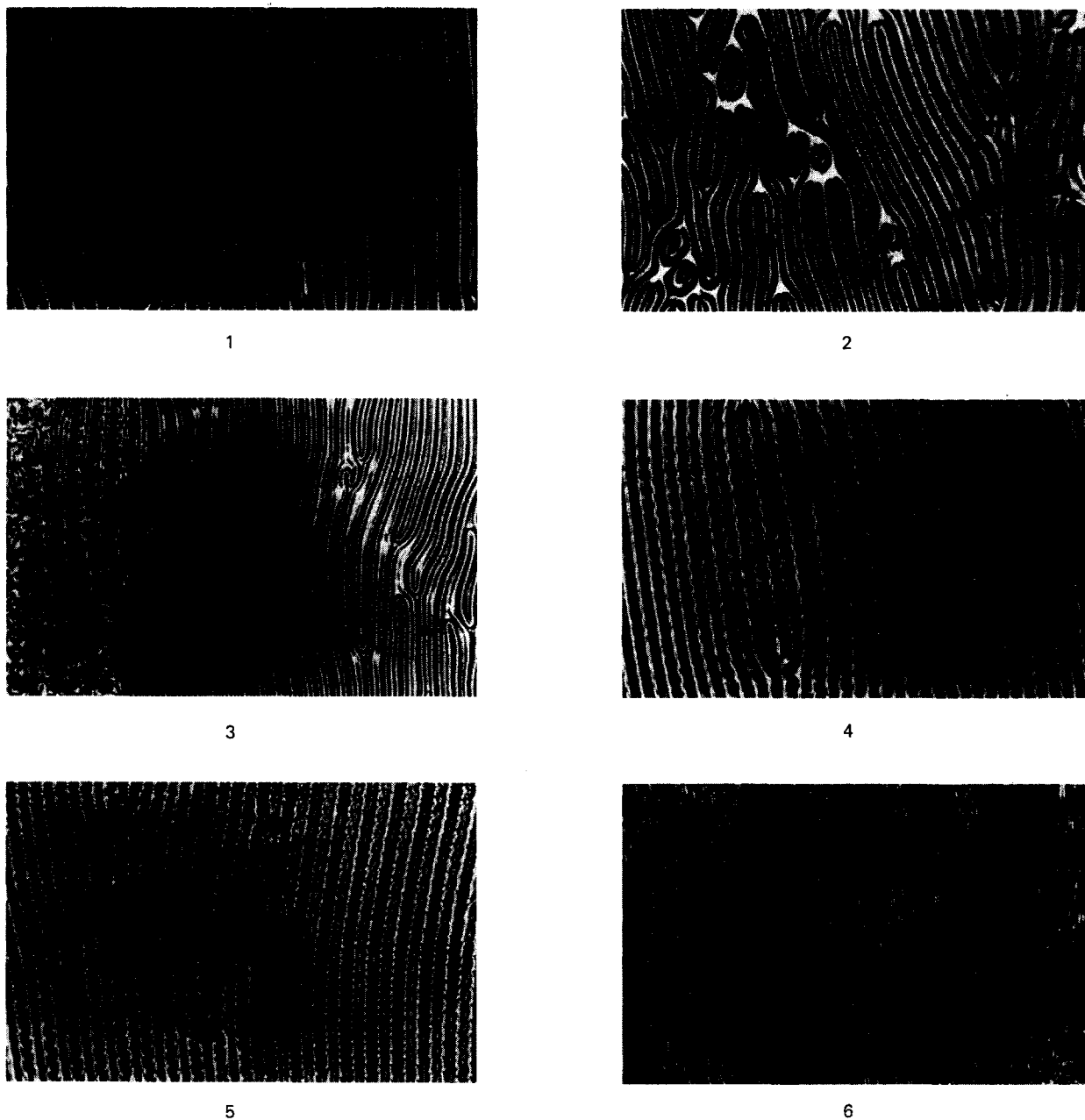


PLATE 9. Photo 1 shows a region of striped inversion walls at 17 V in a $50\ \mu\text{m}$ a -type sample; ppd P, pll A. The photo shows a region 1.3 mm across. Photo 2 shows the stripes of the photo 1 after relaxing to a striped pattern of inversion walls of the Néel type when the voltage is suddenly switched off. Photo 3 shows stripes of Bloch type walls (twist inversion walls) formed from the stripes in photo 1 at 20 V (pll P, pll A). Photos 4 and 5 show interference waves excited by oscillatory motion of the Bloch wall stripes at 35 V in the same sample. These interference waves are of a spatial coherence of the order of the lengths of the stripes which terminate in singularity lines. Exposure time is 1/50 s. Photo 6 shows longer spatial coherence waves in the sample at 35 V, as seen when the instability pattern is slightly out of focus.

lengths. Photograph 1 Plate 9 shows the general aspect of these stripes at 17 V in a $50\ \mu\text{m}$ sample (ppd P, pll A). The width of the stripes (twice the distance from the border to the middle line), is approximately equal to the sample thickness. When the electric field is suddenly turned off, a relaxation process occurs in the first few seconds. This process changes the features of the stripes without changing the overall shape. The changed image of the stripes persists for a few minutes more (photograph 2 Plate 9; pll P, no A). The images of the stripes are seen to be shrinking in length until

they disappear; the two ends approach and annihilate when they meet. A closer inspection of the dark lines bordering these images of the stripes reveals that they are schlieren brushes ending in singularity lines (or as sometimes called "singularity points") of strength $S = \pm 1$.²¹ This means that each such image of a stripe consists of a pair of inversion walls of the Néel type,^{22(a)} almost parallel to the x direction and ending together in singularity lines of strength $S = \pm 1$. We did not investigate if the Néel walls are present in the stripes at this voltage (17 V) or are formed from other types of in-

version walls only after the electric field is turned off (since we believe it happens at higher voltages, 20–50 V).

Typically the regions with this type of striped pattern contain a large number of singularity lines (or “singularity points”) in which the stripes terminate. As it happens in the zero field case, the singularity lines attract or repel each other, causing elongation of some stripes and shortening of others. Many of the singularity lines are the ends of “defect stripes” (i. e., extra stripes inserted into an otherwise regular region, which is a visual analog to defect rolls seen in the Rayleigh–Benard instability).

An increase in voltage (to ~ 20 V in a $50\ \mu\text{m}$ sample) brings on the appearance of new longitudinal lines inside each stripe, as seen in photograph 3 Plate 9 (pll P, pll A). The characteristic additional lines of the stripes and their termination into disclination lines of strength ± 1 seem good indications that these are twist inversion walls (Bloch Walls)^{22(a), (b)} of the kind called *s* inversion walls by Stieb, Baur, and Meier.^{22(b)}

As the voltage is increased, *thinner* additional lines appear. These additional lines together with the additional lines referred to above, seem to spread out of the lines marking the borders of the stripes and their middle lines when they are brought slightly out of focus. (As one of the border or middle lines is taken slowly out of focus, additional new lines move out and to the side of it.) We understand the creation of the additional lines as the rays converging toward the focal lines (appearing as border and middle lines) being subject to an interference modulation in the transverse direction in some regions slightly out of the focal plane. We note that this interference can be seen because of the presence of substantial regions of bend and/or splay deformations close to the plates; the presence of twists in the mid-region of the sample is insufficient.

At higher voltages (25–50 V), the stripes show oscillatory motion. We have observed two main kinds of oscillatory modes. In the most frequent one, the stripe alternately constricts and expands laterally as the oscillatory wave propagates along it (i. e., the two side borders of the stripes oscillate transversely at a phase difference of 180°). This oscillation of the stripe is of small amplitude only, as can be seen in transmitted unpolarized or reflected polarized light. However the additional interference lines in the stripes which were mentioned above produce large amplitude interference, propagating waves of a variety of shapes when the stripes oscillate in this mode. Three of the many propagating interferences seen are “frozen” in photographs 4–6 Plate 9. These propagating interference patterns are caused, in our opinion, at least partially because of longitudinally propagating director orientational waves, under the excitation of the oscillations of the wall. We suspect that some longitudinal liquid flow along the stripes is present (possibly longitudinal loop flows) having some influence on the patterns.

The wavelengths of the propagating interference modes seen are of the order of $1\text{--}100\ \mu\text{m}$ and the periods, as distinguished by eye, of the order of a fraction

of 1 s to about 1 s. Much shorter periods are probably present since photographs taken at speeds of $\sim 1/50$ s show modes unsuspected from direct visual observation. At the same range of voltage at which these oscillations occur, a turbulent liquid motion is seen at the singularity lines at which the stripes end. Some of the longitudinally propagating interference waves also seem to start at these singularity lines, sometimes ending before the other end of the stripe. This seems to indicate that the oscillatory motions of the stripes and associated orientation waves are occurring under the excitation of the flows at the ends of the stripes.

Other propagating wave interference patterns possessing a much larger spatial coherence than the mean distance between the singularity lines at the ends of the stripes are seen when the sample is taken slightly out of focus. Actually it is observed that the singularity lines at the end of the stripes are scattering these moving patterns. The origin of these patterns is probably different from the origin of the above described oscillations, since it is difficult to imagine how unrelated turbulent motions at the end of the stripes could excite waves coherently over many stripes. Photograph 6 Plate 9 is a rather poor record of one of the above types of waves passing like a solitary “silver shadow” over many rolls (*usually* over many rolls). This feature fails to show up in this photograph which is still the best we could take of this kind of moving pattern. The moving “silver shadow” pattern appears in photograph 6 Plate 9 as bright broken pairs of lines of longitudinal orientation. We suspect that this mode is excited by large scale flows in the sample.

Generally, an increase of the voltage increases the frequency and the amplitude and decreases the wavelength of the constriction–expansion mode of stripe oscillations. When at 55–60 V the amplitude becomes quite important ($\sim 5\%$ of the stripe width), the stripes will start breaking down and a turbulent movement takes their place.

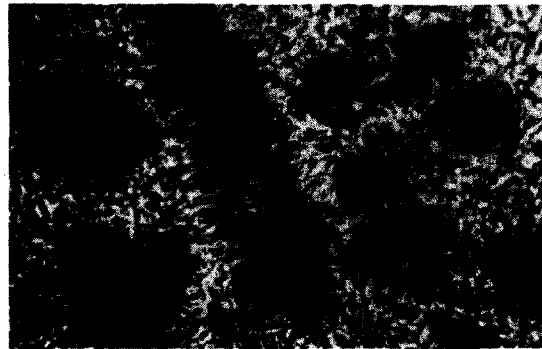
Another kind of oscillation observed only once in our study is similar to the oscillations appearing in the Rayleigh–Benard rolls and mentioned in Ref. 23(a), where the opposite lateral walls oscillate in phase (i. e., an undulatory snakelike type of motion). These oscillations are large amplitude with long wavelength (hundreds of μm) and involve many stripes oscillating together in phase. The period is of a few seconds (25.4 V on a $50\ \mu\text{m}$ α -type sample, SiO evaporated at 4° angle with the plates).

Other often-occurring static or slowly moving variations of this kind of stripe pattern are ones in which in one of the focal planes every second (or every fourth) line is skewed (but now slowly moving). In another focal plane, the stripes (every second stripe, respectively) are divided by transverse lines into rectangular shapes moving in the direction of the stripe; every rectangular shape appears with a spot in the middle.

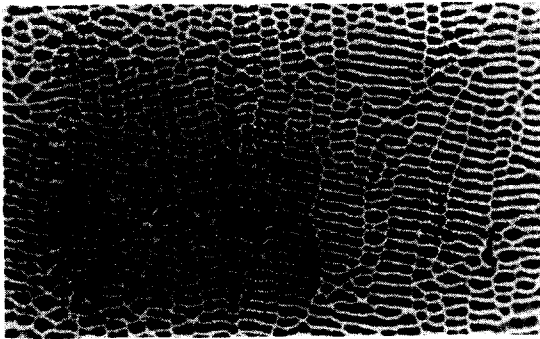
With a little effort (and maybe some imagination too!) the reader might observe in the left upper part of photograph 3 Plate 9 almost (but not exactly) at the corner, another variation of this kind of stripe pattern in which



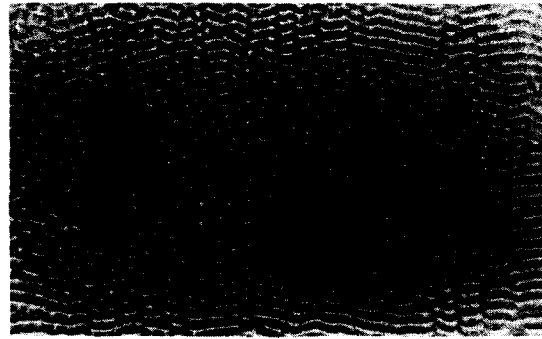
1



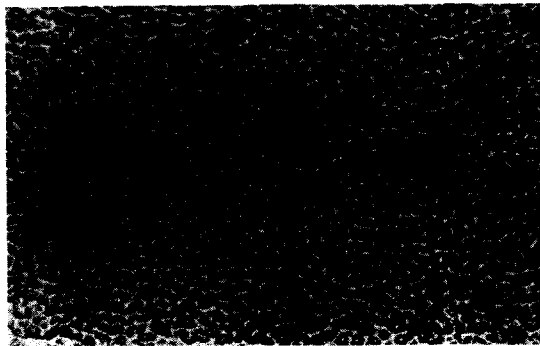
2



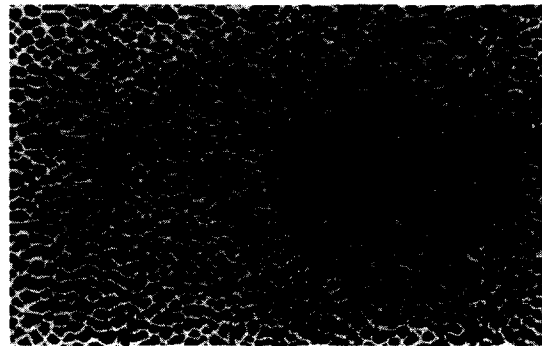
3



4



5



6

PLATE 10. Photo 1 shows inversion regions separated by closed inversion walls and associated with surface coating defects in an $25\ \mu\text{m}$ α -type sample. Photo 2 shows the same region as photo 1 (except for a slight left and upward shift) when a voltage of $40\ \text{V}$ is applied. Turbulent toroidal flows ("rosettes") carrying along nematic threads are formed in the inversion regions. Photos 3 and 4 show the images in two focal planes of an ac conduction regime instability in an α -type sample, $50\ \mu\text{m}$ thick at $11.7\ \text{V}$, $10\ \text{Hz}$. The region seen is $0.7\ \text{mm}$ across and the polars are in the pll P, pll A configuration. Vertical stripes of the pattern of $\sim 70\ \mu\text{m}$ width are moving up and down alternately. Photos 5 and 6: Images in two focal planes of an ac conduction instability, $12.5\ \text{V}$, $10\ \text{Hz}$ $50\ \mu\text{m}$, α -type sample.

the central line is "zigzagged", and at each side of it, spots appear alternately at each turn.

Another distinct EHD encountered consists of a toroidal flow carrying along nematic threads. Because of this, it has the aspect of a rosette. Photograph 2 Plate 10 shows a few such "rosettes". The central flow appears to move from the positive plate towards the negative one. At voltages of ~ 20 – $80\ \text{V}$, such a flow is confined to places where at zero field the nematic shows

orientational distortions, particularly areas where the xy plane projection of the nematic director is inverted or almost inverted with respect to the bulk (with inversion wall separation). These inversion areas are anchored at sites of defects in the surface coating and are usually field induced. In the thinner samples ($25\ \mu\text{m}$) some inversion areas will persist for long times after the field is switched off. Photograph 1 Plate 10 shows the zero field aspect of inversion areas at which the "rosette" flows of photograph 2 on the same plate oc-

cur when the voltage is applied. (The two photographs are taken at slightly different positions.) The speed of the flow, the apparent turbulence, and the density of the nematic threads carried by the "rosettes" increases with voltage. Although highly turbulent, some molecular alignment exists in these flows even at the highest fields tried (80 kv/cm on a 50 μm sample). The insides of the "rosettes" possess a main birefringence direction, punctured by fluctuating spots of other birefringence directions. At voltages of about 60 V in 50–75 μm samples, nematic droplets of different birefringence directions than the surroundings and nematic threads are seen to be ejected from the "rosettes." Starting at ~ 80 V the "rosettes" begin forming on their own, at places showing no apparent distinction in the absence of the field.²⁴ Over about 100 V in some regions of the samples the "rosettes" form dense populations and pack into polygonal patterns (Plate 12 photograph 5). The polygonal flows are seen to jump apparently randomly from place to place (characteristic time between jumps ~ 1 s); in particular, polygon vortices are observed to become new polygon centers. Apparently the lower voltage behavior by which the flow in the middle of the "rosette" moves from the positive to the negative plate is not followed any more. This polygonal grid of flows is probably related to the spoke pattern of the Rayleigh–Benard type of flow described by Busse and Whitehead.^{23(a),(b)} Once one becomes accustomed to the shape of the "rosette," one can recognize this kind of flow while it makes brief appearances (of a fraction of a second) in regions of intense ("homogeneous") turbulent flow. It may be that at certain voltages, the difference between regions showing a grid of polygonal "rosettes" and the regions of turbulent flow is that in the former there are enough surface defects to stabilize the grid. This could possibly be checked by controlling the density of defects. Usually at about 60 kv/cm the "rosette" grids recede to regions near the walls, and the VGMV expands over most of the sample.

Over ~ 80 V (as for a ~ 75 μm sample), the "rosettes" associated with surface coating defects and side walls are clearly seen to participate in sustaining flow motion of masses of adjacent liquid. At very high voltages (300–400 V), these flows can extend many mm into the samples which at these voltages are covered mainly by the VGMV. Fronts of defects in the variable grid modes variant are seen being radiated from the "rosettes." Usually these fronts of defects propagate smoothly, but sometimes they move in a jumpy, pulsating mode (period ~ 1 s). The defects in the front are of the kind that puncture the pattern shown in photographs 3 and 4 Plate 8, (i.e., ends of defect stripes). Photograph 6 Plate 12 shows such an occurrence. The "rosette" region seen dark and blurred is at the bottom of the photograph, and the fronts of defects are seen as what looks like "field lines" around the "rosettes" and extending away from them (upwards in the photograph). The photograph fails to show the VGMV pattern which was visible to the eye when the picture was taken. The stripes of the pattern were in this case approximately perpendicular to the front lines of the propagating defects. The region shown by the photograph is about 0.7 mm across.

3. Samples prepared for planar alignment at low dc voltages

75 μm samples made from (not specially cleaned) Nesatron glass showed at ~ 10 V dc predominantly a coexistence of hexagonal pattern areas (as in *p*-type samples) and replicating instability pattern areas (as in the *a*-type samples).

In 50–100 μm samples with the glass surface prepared for planar alignment by SiO evaporation at $\sim 30^\circ$ and at ~ 10 V dc, the predominantly encountered figures were inversion walls of the types described in Ref. 22(b).

4. Additional comments and observations

In the following we give our further thoughts about some of the phenomena seen by dc excitation, trying to offer intuitive explanations whenever possible.

We start with the low voltage (7–15 V) *a*-type sample instability (cf. Sec. IIIB 2a and Plates 3–7). We see the formation of the incipient flow at a nematic distortion as a focalization effect, the distortion lowering the voltage threshold for the formation of Felici-type loops of flow. (Similar effects have been observed in the related Benard convection in nematic experiments in which convection loops nucleate around "defects of structure."²⁵)

The loop flow assumption is supported by observations of dust particle movements which, as is well known,²⁶ are induced by liquid flows. At this stage these observations are not very extensive. However, we have observed loop movement of dust particles in the core flow. With reference to photograph 5 Plate 7, these loops extend radially from the central region of a core flow (where the movement is perpendicular to the plates), to a region close to the bright closed rounded curve delimiting the core flow (where the movement is again perpendicular to the plates). This describes the loops as seen in a moving frame attached to the flow figure; by "central region" we mean a small region in the center of the core flow. Most of the dust particles which move on a loop extending up to the closed bright curve will remain entrapped in the flow for many cycles (period ~ 1 s in a 90 μm sample at 11 V). The dust particles moving on a trajectory which brings them to the bright closed curve will either escape smoothly from the core flow, or will be violently accelerated and thrown out of the bright line region (this is seen only in good quality samples which show replication and regular grids). There is an apparent contradiction in the fact that sometimes the dust particles will pass the bright closed lines (which represent walls) and be unaffected, and sometimes will violently interact with these walls. At this stage we think that there is a region close to one of the plates in which the wall does not penetrate or is broad and not very "dense" and through which the dust particles can pass unaffected. The way the bright closed curve interacts with the dust particles indicates that it is of a nature similar to the bright lines delimiting the stripes in the VGMV instability discussed in paragraph 2b of this section. Another indication was noted in

paragraph 2b in connection with the unfolding process. In the context of the Felici and Carr models, we understand the bright closed rounded curve as representing a cylindrical "Carr wall" focalizing a strong charge and mass flow which brings the injected charge to the opposite electrode. The wall acts as a pump "sucking" masses of charged liquid around its base near one of the electrodes and ejecting it at the other electrode. Here the flow is depleted of the charges and splits into two parts which move parallel to the plates, one towards the interior of the cylindrical wall and one towards the exterior. The part moving toward the interior is forced to move downwards by a similar flow coming from the diametrically opposed directions, continues back to the injecting electrode and is recycled. This corresponds to the closed loops of the core flow which we observed by dust particle movement. The part of the flow which moves towards the exterior of the cylindrical wall is not constrained to bend back and probably disperses (in the sense that it forms a much slower loop branch of a much larger section). Thus the loops oriented toward the exterior of the wall can be practically seen as incomplete, "[]-shaped. We do not have at this stage direct evidence of this kind of "incomplete," external loops from dust particle observations. (Dust particles are seen to move in the regions external to the cylindrical wall, sometimes away from the wall and sometimes toward the wall. Still we cannot affirm that we have yet seen these incomplete loops; we only infer that they exist.) The branches are supposed to be "Carr walls" also and to support such incomplete loops on both of their sides. The wakes of the flow figures (cf. Sec. III B 2a) can be an indication of such incomplete loops. These are regions where the director is no longer in the xz plane. Such distortions can be formed by a velocity gradient dv_x/dz [cf. Ref. 12(c)] which can be indicative of the supposed "incomplete" loop flow. Back flows that follow the moving distortion, and could be suspected as the reason for these dv_x/dz gradients, can be ruled out if we are right in identifying an EHD we observed as being "flow figures without core flows" (Sec. III B 2a), since in their *static* version these show regions of this type (two or four spots in which the director is out of the xz plane).

The two branches attached to the flow figures could be seen as induced by the "incomplete" loop flows, external to the cylindrical wall. The reason we think this happens is explained below. We consider these flows to be in a first-approximation "incomplete" loop flows spreading radially around a cylindrical wall at which the flow is in the z direction. We now consider the director bending caused by each loop of flow. Starting with the loop in the $+x, +z$ quadrant of the xz plane and increasing the angle ϕ between the loop plane and the x direction, we see that at some angle, the bending should change direction. If initially the director is parallel to the x axis, then the change in the direction of the bending induced by the flow occurs at the loop flowing in the yz plane ($\phi = 90^\circ$). For oblique orientation of the director, we expect the direction of the bending to change at a $\phi > 90^\circ$ or $\phi < 90^\circ$, depending on the orientation of the director with respect to the velocity gra-

dients in the loop flows. This could explain the formation of the two branches oriented backwards at an angle with respect to the moving direction of the grid of flows, as being induced by this change in bending direction.²⁷ As explained previously, the two branches have optical properties corresponding to a "heap" in the director direction (i. e., a changing of the tilt direction in the xz plane by a splay-bent distortion). The fact that the two branches seem to extend out of the regions in which there is an "external" loop flow supported by the cylindrical wall could be explained if we remember that at higher voltages moving walls of tilt inversion seem to form even before the flows form. These could be an EHD of whatever type or a flexoelectric instability, the threshold of which is above the threshold of the flow figures. The extension of the branches out of the region of the flow supported by the cylindrical wall could be seen as caused by the excitation by the above change in bending direction, of a flexoelectric or an EHD instability mode in a subcritical regime (to make use of the analogy between onset of instabilities and phase transitions). After their excitation, these modes transform into Carr walls by a mechanism similar to the one suggested by Carr, by which Williams domains give rise to this type of wall (cf. Refs. 16). In their turn, the branches are seen as loop flow focalizing structures, and the new core flows will appear preferentially on the branches.

It is not clear to us the extent to which fluctuations on the branches play a role in the focalization of the core flows. Some flickering in the branches seems to indicate strong fluctuations in these regions. Why the flows tend to be created at certain sites and then keep a precise distance between them, and why at higher voltages the flows will divide and unite might be seen as a question of the structure of the branch modes on which the flows focalize and of how core flows interact (mainly through the branches), and we cannot yet offer an answer. Since according to the Carr model^{16(a)} the flows in the walls cause charge accumulation, electrostatic forces could play a role.

The present explanation implies that the flows supported by the cylindrical wall induce two additional distortions (of a twist type) one preceding and one following the cylindrical wall. A weak distortion is seen preceding the cylindrical wall but none is seen following, presumably because of the presence of the nearby flows supported by the branches. The movement of the flow figures as a whole are possibly due to the propagation of the nematic distortion of the wall structure mainly under the elastic torques in the nematic. These propagating distortions are possibly of a solitonic character as seems to be indicated by the solitary movement propagation of the flow figures. The wavy character of the nematic distortions in the wakes of the flow figures are reminiscent of the wave trains accompanying solitons in some cases.

The p -type cell converging pattern as shown in photograph 4 Plate 1 and consisting of two families of parallel lines which intersect at the hexagonal flow centers can be explained by the same kind of qualitative reason-

ing. At this stage, we want to point out that as yet we have not carried out dust particle movement observations in p -type samples, but we strongly believe that the hexagonal instability actually involves loops of liquid flows.^{20(a)} Although below we suppose that the flow distribution is similar to the one in the hexagonal Benard cell, it might not necessarily be so.²⁶ We assume that the flow has the tendency to have a cellular but not roll-like form, as seems to be the case when charge injection is involved,²⁹ and, as known to be possible, when there is some asymmetry with respect to a reflection about the middle plane of the conductive layer. We consider the flow to be toroidal in a first approximation (this time composed of loops of flows spreading circularly around a common central part at which the flow is in the z direction). In the p -type samples, the director exhibits two directions of tilt along the same vertical to the plates [e.g. cf. Fig. 1(a)]. A toroidal flow which will tend to form, will change the tilt direction in this case at two different values of ϕ (viz., one $> 90^\circ$ and one $< 90^\circ$) at two different levels of z . We may attribute the formation of the two families of parallel lines in the pattern to the existence of these two changes in tilt directions. If these play the same role in focusing the flow as the branches of the a -type samples seem to play, then the hexagonal pattern formation in this case would likely require a special set of circumstances to form. This is because the angle between the two families of distortions in which the tilt direction changes is a function of many parameters like the initial tilt of the director at the plates, the nematic elastic constants, Leslie's viscosities and dielectric anisotropies. Then, in order to allow the 60° angle necessary for the hexagonal pattern to be a stable distortion, the values of each of these parameters would have to be within a small range. Moderate changes in these parameters would be expected to just distort the pattern of regular hexagons until large enough changes are made which could lead to new patterns, as could be the case of the rhombic pattern in our aged p -type samples [cf. Secs. III B and III C].

The movement of the hexagonal pattern as a whole in the $\pm x$ directions could be explained as the result of some incidental asymmetry between the lower and the upper part of the sample (possibly related to the unipolar charge injection), making the p -type sample a "little more" a -like, and thus having a movement for reasons similar to those we suggested for the a -type samples. The fact that the hexagonal image of the pattern is divergent (e.g., picture 2 Plate 1) could be explained if, instead of having the configuration of Fig. 1(a) with a discontinuity in director orientation midway between the plates, the line of director orientations forms a smooth C-shaped curve with no such discontinuity [This would imply that the director is oriented perpendicular to the plates midway between them instead of parallel as shown in Fig. 1(a)]. This could be the distribution for Phase V at zero field or it can happen under the influence of the field. We have not yet been able to investigate this matter.

The VGMV creation after the low-voltage dc instabilities break down is seen as the transition from a regime

dominated by an unipolar charge process to a bipolar regime. Under the conditions in which the VGMV was observed in our samples, one would expect the dc version of the "ED" instability of Ref. 12(b) to occur, at least at low voltage. We think the two instabilities are different, the VGMV apparently involving walls and shear flow alignment. This could be an indication that the presently used material possesses properties which facilitate the formation of Carr walls at lower voltages. In view of our lack of experience with the ED instability of Ref. 12(b), and in view of the compactness of the descriptions in this reference, it seems desirable to investigate this matter more.

We wish to point out that although the present explanations relies heavily on the existence of Carr walls we see no reason to rule out flexoelectric contributions to the above phenomena.

C. AC conduction instabilities

Williams domains were most frequently encountered patterns below ~ 9 V, but we also observed some three-dimensional patterns in the ac conduction regime at higher voltages. At about 11 V a "zigzag roll" pattern is often seen (Williams domains zigzagged at 120° – 150° angles). Typical three-dimensional ac conduction instability patterns observed in our samples are shown in photograph 6 Plate 2 and photographs 3–6 Plate 10, all taken with pll P, pll A. Photographs 3 and 4 Plate 10 are the images in two different focal planes of an instability appearing at 11.7 V, 10 Hz in an a -type sample of $50 \mu\text{m}$ width. The region shown is ~ 0.7 mm across. There is a movement in this pattern in which vertical stripes ($\sim 70 \mu\text{m}$ width) move up and down alternately. This pattern is basically a zigzag roll pattern broken into moving stripes. It could be interesting to investigate whether this type of motion is not associated with striped liquid mass flow of the kind to be described below in relation to the moving chevron pattern. Photographs 5 and 6 of the same plates are images in two different focal planes of an instability at 12.5 V, 10 Hz in the same sample.

A feature often encountered in our samples in the ac conduction regime is the cross-roll instabilities. These are oscillatory back and forth reformations of a roll pattern in two different orientations [i.e., a region of rolls of a particular orientation loses its ordered appearance (or changes into a nonroll pattern region) only to rearrange itself again into a region of rolls of a different orientation, the process being repeated back and forth between the two orientations]. This kind of behavior is well-known to exist in the Rayleigh-Benard type of experiments at moderately high Rayleigh numbers.^{23(a),(c)} (But we do not wish to imply that the cross rolls in our samples necessarily have the same origin.)

Photographs 1, 2, 3 Plate 11 showing a region with cross roll in a $50 \mu\text{m}$ p -type sample at 10 V, 4.5 Hz are taken at the same position at 0.25 s intervals. The oscillation period is 0.5 s. Note the division of the cross-roll area shown by the photograph in regions oscillating at different phases but with almost the same period. The rolls, of a width approximately equal to the width of the sample, are seen crossing at an angle of

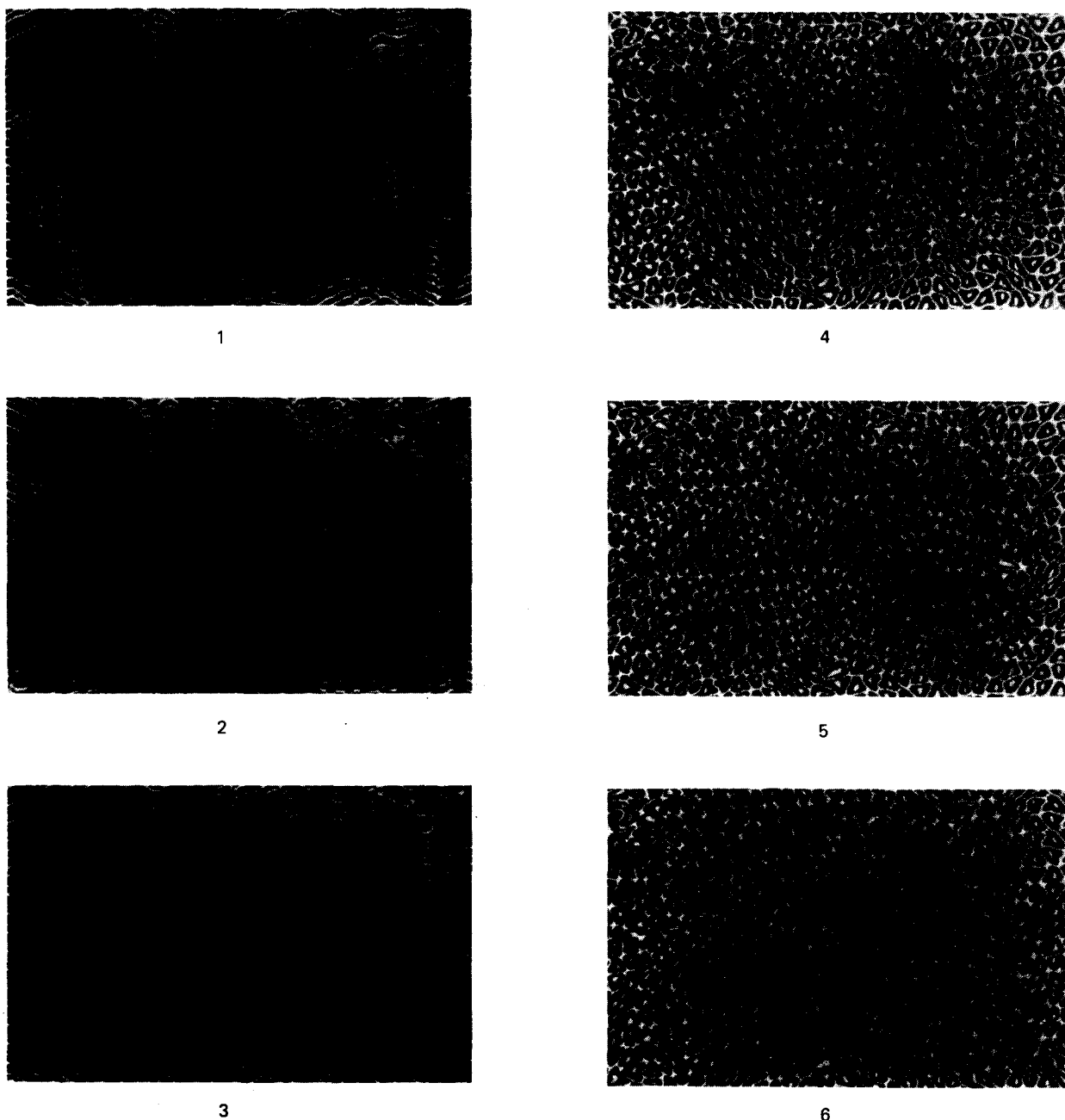


PLATE 11. Cross-roll instabilities (ac conduction regime). Photos 1-3 show 120° cross roll in a $50\ \mu\text{m}$ p -type sample at 10 V, 4.5 Hz. The photos were taken at 0.25 s intervals, while the period is 0.5 s. The area of the sample seen in the photos is divided into regions of rolls of different orientation. In each region rolls are formed periodically in one of the two different directions. This is not a rotation of the rolls as can be inferred by looking at the photographs. Photos 4-6 show a variation of the cross roll instability in which there is an intermediate stage of triangles. Regions in photos 4 and 6 show the two extremes, while in photo 5 the same regions display an intermediate triangular pattern. The rolls are seen to preserve some features of the shape of the triangle flows. The period is ~ 1 s and this was seen at 8.4 dc in a rubbed sample.

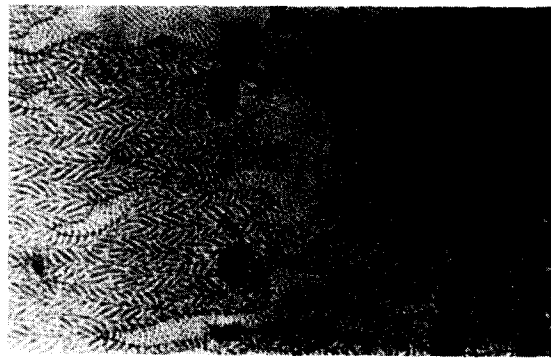
120° . The period of the crossing decreases as the voltage is increased, and after further voltage increase, turbulence follows. Usually when cross rolls occurred in one of our samples, only parts of it would exhibit this instability; other regions display almost static rolls or turbulent motion.

Photographs 4, 5, 6 Plate 11 show a type of cross roll which occurs via an intermediate state in which a cellular pattern of triangles is formed (10 V, dc in a rubbed $75\ \mu\text{m}$ sample). The period was ~ 1 s. It might be ob-

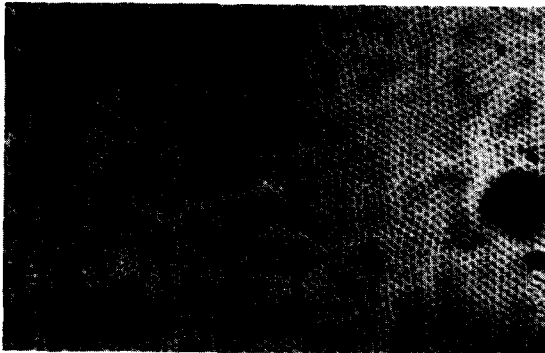
jectionable to classify this last instability as a cross roll. The reason we do this is because the oscillations are between two patterns appearing to have much of a roll-like character. The rolls in this case are not as straight as the ones in photographs 1, 2, 3 Plate 11, and they are seen to preserve some "memory" of the triangles out of which they evolve. Each of the triangles is a flow composed of several components (three being predominant). The stripes in the pattern are formed when the same mode component of each triangular flow becomes predominant, coherently over stripes of tri-



1



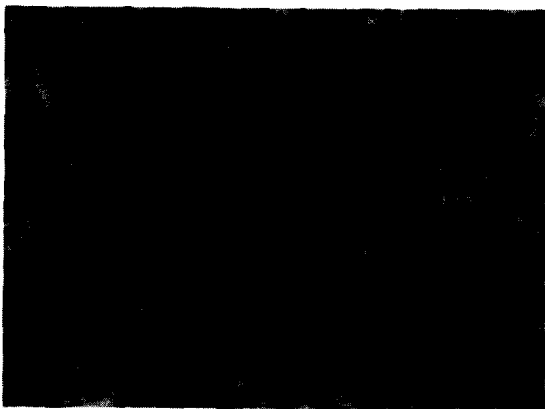
2



3



4



5



6

PLATE 12. Photo 1 shows the horizontally moving (y direction) chevron pattern in a $75 \mu\text{m}$ a -type sample under 75 V, 150 Hz. The moving chevrons are associated with liquid flow of similar trajectory. Snakelike figures bordered by threads adhering to the upper and lower plates are seen to move in a snakelike motion. One of the snakes is seen just above the middle of the photograph spreading from left to right. Usually the pattern inside the snake in a -type samples is like the "snake skin" seen in regions between the moving chevron pattern of photo 2, or as shown in more detail in photo 3. Photo 4 shows an alternate skew-straight pattern (35 V in a $75 \mu\text{m}$ sample) with bright spikes at the vortices, where the zigzags break and curl at about 50 V. Photo 5 shows a polygonal grid of turbulent flows ("rosettes"); 100 V on a $50 \mu\text{m}$ a -type sample. The photograph shows a region ~ 0.7 mm across. Photo 6 shows a typical occurrence at 300 V in a $50 \mu\text{m}$ a -type sample. In the lower part is seen a region of rosette-like turbulent flows occurring near a side wall (dark and diffuse). The upper part is a region of a variable grid mode stripes which fails to show up in the photo, although visible to the eye when the picture was taken. Defect fronts in the stripes (seen as curvy parallel lines that look like field lines in the photograph) are observed to radiate out, along the stripes of the variable grid mode almost normal to the "field-lines" which are in a jumpy, pulsating mode (period ~ 1 s).

angles. As inferred from the stripe patterns, they seem to have a roll character. In some cross-roll instabilities occurring via a cellular nonroll intermediate, which were slow enough for adequate dust particle ob-

servation, we could actually follow this type of behavior of flow components becoming coherently predominant over stripes. The intermediate cells unite together to form rolls each time the predominant flow is in the right

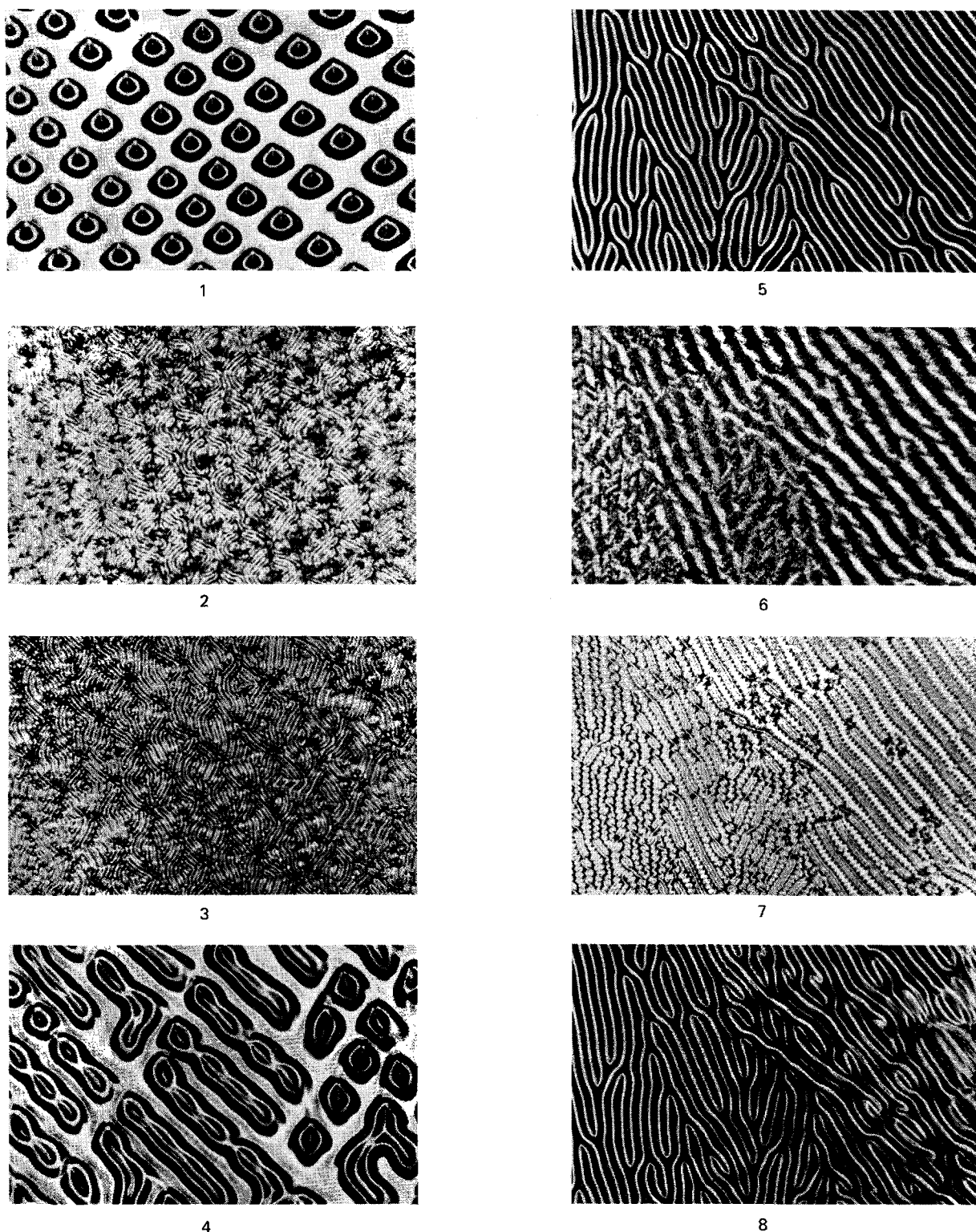


PLATE 13. Examples of the processes of folding and unfolding when the voltage on the sample is suddenly increased to a value at which a variable grid mode variant exists. The walls normally delimiting the stripes will skewbend into different shapes depending on the initial conditions (folding). Photos 1 (11.2 V dc, $50\ \mu\text{m}$ α -type sample) and 5 (35 V dc, sample) show the initial patterns leading to the creation of the patterns of photos 2 and 6, respectively, after a sudden 100 V increase in the voltage. When the voltage is then lowered (at a ~ 10 V/s rate) a process of unskew-bending (unfolding) takes place, leading to the approximate reformation of the patterns existing before the sudden voltage increase. This is illustrated by photos 3 and 4 showing stages in the unfolding of the pattern of photo 2, and by photos 7 and 8 showing stages in the unfolding of the pattern in photo 6.

direction. At the time of writing we are not sure that the triangular intermediate cross roll is an ac conduction instability or a dc instability. Another ac conduction

regime cross roll observed in an aged p -type sample, with rolls crossing at 120° occurred via a hexagonal intermediate pattern. Related phenomena are described

by Quon and Wiener-Avneer³⁰ and by Manneville³¹ who cites a work in preparation by Ribotta.

D. Alternating-current dielectric instabilities

The most commonly encountered ac dielectric instability pattern in our a and p -type samples was the chevron pattern.^{2,4(c)} At a few volts over the threshold for the formation of the chevrons, movements in the pattern start occurring. Similar observations have been made by many authors on samples oriented for planar alignment of different nematics [See for example Ref. 4(c)]. In our samples the movements occurred in stripes, oriented approximately either parallel or perpendicular to PIDAP, the movement of each stripe being opposite in direction to the movement of the adjacent stripes. Photograph 1 Plate 12 shows a chevron pattern in a region ~ 0.7 mm across formed in a $75 \mu\text{m}$ a -type sample at 75 V, 150 Hz. The initial orientation of the director in the sample is in the xz plane [Fig. 1(b)] which intersects the photograph image vertically. The movement of the stripes occurring in this sample was mainly in the horizontal y direction. A moving stripe in this type of moving chevron pattern has its center on the line at which the little curvy striations (a few μm thick) of the pattern converge at an angle (the little closed dark curve situated slightly lower than the center of the picture is oriented along such a middle of a stripe). The direction of motion of each stripe is opposite to the direction that the acute angle formed by the striations points to. The border lines of the moving stripes are, naturally, in the middle between two such lines. Because of this movement, the little striations break into two halves which rejoin periodically into new striations along these border lines. Observation of movement of dust particles in our samples show that the movement of the chevron stripes is associated with stripes of identical delimitation of liquid flows having the same velocity. At the side wall of the sample, the stripe of flow divides into two parts which turn around on both sides to become halves of the adjacent stripes. Thus, there is an overall liquid flow pattern in the whole, or large parts, of the sample that is associated with the chevron pattern movement (i. e., on an xy plane loop pattern). This simple mode of flow we describe is not realized in practice without distortions and defects. (Actually photograph 1 Plate 12 is of a quite imperfect pattern.) The defect most often encountered is when stripes moving in opposite directions collide head on. When this happens both stripes divide into two branches. The two branches of one stripe continue in the same direction by surrounding the other stripe while the two branches formed by the latter fold back and aside to join the flow of the two branches of the former (i. e., an extra pair of loops inserted part of the way into an otherwise regular pattern distorts the pattern by pushing aside part of two adjacent loops). When the moving chevron pattern is taken slightly out of focus, one loses the details of this pattern, but instead the contours of the flow pattern may be observed. The diverse forms of the flow pattern bear a striking resemblance to some of the various forms of the VGMV described above, paragraph B2b (the alternate skew-straight pattern for example is often seen).

A striking occurrence in our samples at voltages high above the threshold for chevron formation (15–20 V above) is a moving, snakelike (or sluglike) figure. One such “snake” is seen in photograph 1 Plate 12, above the middle, in the center and to the left. The “snake” originally created at the left wall was moving in a typical snakelike movement from left to right when the photograph was taken. This y direction movement is related to the underlying stripe mass flow which probably drives the motion of the “snakes.” In chevron patterns with vertical (x direction) stripe motion the “snakes” move vertically. The lines by which the “snake” is bordered are surface disclination lines (adhering threads)²¹ attached to the upper and lower plates (the thicker line on the top of the long “snake” of photograph 1 Plate 12 is the thread attached to the upper plate, the thinner one is attached to the bottom plate). The two threads adhering to the plates are connected in most of the cases by vertical or short inclined bulk threads. The thread contouring the long “snake” of photograph 1 Plate 12 was part of a thread originally formed in a strong flow of narrow delimitation streaming along the side wall. (Such flows along side walls were occasionally encountered in a -type samples at practically all the frequencies studied, 0–300 Hz.) The thread was attracted into the flow associated with the moving chevrons with which the flow occurring along the side walls interacts. Other threads contouring observed “snakes” were seen originating at irregularities associated with wall and surface coating defects.

In most of the cases, in a -type samples the “snakes” are seen to possess a real “snake skin” (i. e., the pattern seen between the bordering surface disclination lines differs from the surrounding chevron pattern). For most of the thin “snakes” that appear at first when sufficient voltage is applied the “snake skin” appears as a fracturing of the surrounding chevrons, and they show some continuity with the chevrons (as can be seen in the case of the long snake of photograph 1 Plate 12). However, as the voltage is increased, the “snakes” become bulkier, and the pattern inside and away from the disclination lines looks unrelated to the chevron pattern. This situation is illustrated in photograph 2 Plate 12 where a chevron pattern is shown in coexistence with bulky, slowly moving snakes, and with a large region covered with the snake-skin pattern. Eventually further increase of the voltage induces formation of large regions of “snake skin” patterns in which “snakes” confining the chevron pattern are now seen moving. A more detailed photograph of the snake-skin pattern is photograph 3 Plate 12. Sometimes this pattern looks hexagonal.

Finally, we offer a few words about dark spots seen in our samples and often appearing in photographs of chevron patterns published by various authors but apparently not given much attention. Three such spots are seen in photograph 2 Plate 12 in the right lower corner. These spots, appear dull and dark in the pll P, pll A configuration, but become bright, real “fireballs” (with a dark center) at high magnification and ppp P, pll A. They exhibit “fast turn off” (cf. Sec. I) and have some features which seem to relate them to the high

voltage dc EHD described above as looking like rosettes. As in the case of the "rosettes," when the voltage is increased, these spots first appear at distortion sites in the nematic occurring at obvious defects in the surface coating, and at higher voltages they start appearing at sites of no obvious distinction. The number density of these spots increases with voltage. We have observed sites of high density of these dark spots, but not dense enough to possibly form a close-packed grid as in the case of the "rosettes." Under crossed polarizers, the spots appear as sites of high agitation, ejecting nematic threads and nematic droplets of other orientation than the surroundings. Although quite stable, the spots are seen to make very small, sometimes jumpy excursions about their most preferred site.

It seems probable that a way could be found to control the surface defects on which the spots nucleate (using for example photographic etching methods³²). In view of their fast turn off, the spots might find application in display devices using surfaces thus prepared for creation of arrays of spots.

ACKNOWLEDGMENTS

We wish to thank Dr. Jing-Huei-Chen for first pointing out to us the novelty of our early observations. We wish to thank Professor P. G. de Gennes for an early encouraging conversation. We especially wish to thank Denise E. Freed for her help with some of the observations reported here, in particular for first observing and photographing the instability of Plate 11, photos 4-6. We thank Professor James T. Jenkins for his sustained interest in this work and for a critical reading of the manuscript.

¹R. Williams, *J. Chem. Phys.* **39**, 384 (1963).

²A good review which summarizes basic theory and experiment of EHD's in liquid crystals and other phenomena related to our study, T. J. Scheffer and H. C. Grüler, in *Molecular Electro-optics*, edited by C. T. O'Konski (Dekker, New York and Basel, 1978), Part 2, Chap. 22.

³W. Helfrich, *J. Chem. Phys.* **51**, 4092 (1969); **52**, 4318 (1970).

⁴(a) Orsay Liquid Crystal Group, *Phys. Rev. Lett.* **25**, 1642 (1970); (b) E. Dubois-Violette, P. G. de Gennes, and O. Parodi, *J. Phys. (Paris)* **32**, 305 (1971); (c) Orsay Liquid Crystal Group, *Mol. Cryst. Liq. Cryst.* **12**, 251 (1971).

⁵See, for example, (a) P. A. Penz and G. W. Ford, *Phys. Rev. A* **6**, 414, 1676 (1972); (b) T. O. Carroll, *J. Appl. Phys.* **43**, 1342 (1972); (c) E. Moritz and W. Franklin, *Mol. Cryst. Liq. Cryst.* **40**, 229 (1977).

⁶(a) N. J. Felici, *Rev. Gen. Electr.* **78**, 717 (1969); (b) J. Phys. (Paris), **37**, C1-117 (1976).

⁷E. F. Carr, *Mol. Cryst. Liq. Cryst.* **7**, 253 (1969).

⁸P. G. de Gennes, *The Physics of Liquid Crystals* (Clarendon, Oxford, 1974).

⁹G. H. Heilmeyer and W. Helfrich, *Appl. Phys. Lett.* **16**, 155 (1970).

¹⁰(a) M. I. Barnik, L. M. Blinov, M. F. Grebenkin, and A. N. Trufanov, *Mol. Cryst. Liq. Cryst.* **37**, 47 (1976); (b) M. I. Barnik, L. M. Blinov, S. A. Pikin, and A. N. Trufanov, *Sov. Phys. JETP* **45**, 396 (1977).

¹¹E. Guyon, P. Pieranski, and M. Boix, *Lett. Appl. Eng. Sci.* **1**, 19 (1973).

¹²(a) S. A. Pikin, V. G. Chigrinov, and V. L. Indenbom, *Mol. Cryst. Liq. Cryst.* **37**, 313 (1976); (b) S. Pikin, G. Ryschenkov, and W. Urbach, *J. Phys. (Paris)* **37**, 241 (1976); (c) P. Pieranski, E. Guyon, and S. A. Pikin, *ibid.* **37**, C1-3 (1976).

¹³(a) R. B. Meyer, *Phys. Rev. Lett.* **22**, 918 (1969); (b) Yu. P. Bobylev and S. A. Pikin, *Sov. Phys. JETP* **45**, 195 (1977).

¹⁴(a) L. K. Vistin, *Soviet Phys. Crystallogr.* **15**, 514, 908 (1970); (b) M. I. Barnik, L. M. Blinov, A. N. Trufanov, and B. A. Umanski, *J. Phys. (Paris)* **39**, 417 (1978); *Sov. Phys. JETP* **46**, 1016 (1977).

¹⁵(a) W. Greubel and U. Wolff, *Appl. Phys. Lett.* **19**, 213 (1971); (b) P. K. Watson, J. M. Pollack, and J. B. Flannery, in *Liquid Crystals and Ordered Fluids*, edited by J. F. Johnson and R. S. Porter (Plenum, New York, 1978), Vol. 3, p. 421.

¹⁶(a) E. F. Carr, in *Liquid Crystals and Ordered Fluids III*, edited by J. F. Johnson and R. S. Porter (Plenum, New York, 1978), p. 165; (b) E. J. Sinclair and E. F. Carr, *Mol. Cryst. Liq. Cryst.* **37**, 303 (1976); (c) E. F. Carr, P. H. Ackroyd, and J. K. Newell, *Mol. Cryst. Liq. Cryst.* **43**, 93 (1977); (d) C. E. Tarr and E. F. Carr, *Solid State Commun.* **33**, 359 (1980).

¹⁷G. H. Heilmeyer, L. A. Zaroni, and L. A. Barton, *Proc. IEEE* **56**, 1162 (1968).

¹⁸(a) W. Urbach, M. Boix, and E. Guyon, *Appl. Phys. Lett.* **25**, 479 (1974); (b) D. Armitage, *J. Appl. Phys.* **51**, 2552 (1980).

¹⁹P. Andrew Penz, *Phys. Rev. Lett.* **24**, 1405 (1970); *Mol. Cryst. Liq. Cryst.* **15**, 141 (1971).

²⁰(a) Direct observations of dust particle movement have confirmed that there is a flow pattern associated with the hexagonal pattern. (b) See, for example, E. L. Koschmieder: *Benard Convection*, *Adv. Chem. Phys.* **26**, 141 (1971).

²¹D. Demus and L. Richter, *Textures of Liquid Crystals*, 2nd ed. (VEB Deutscher Verlag für Grundstoffindustrie, Leipzig, 1980).

²²(a) W. Helfrich, *Phys. Rev. Lett.* **21**, 1518 (1968); (b) A. Stieb, G. Baur, and G. Meier, *J. Phys. (Paris)* **36**, C1-185 (1975).

²³(a) F. H. Busse, *Rep. Progr. Phys.* **41**, 1929 (1978); (b) F. H. Busse and J. A. Whitehead, *J. Fluid Mech.* **66**, 67 (1974); (c) **47**, 305 (1971).

²⁴Usually the rosettes will form in some regions of the samples, and not in others. We think that there must be a distinction between the parts of the sample showing at a certain voltage different dc modes (variable grating variant, turbulence, "rosettes") since the same modes tend to form in the same regions of a sample each time it is tried under the same conditions. The regions showing different modes at high voltages, usually display the same low voltage (≈ 15 V) modes. Surface preparation differences are probably the main reason for the different high dc voltage modes. We suspect also that at these high voltages there are large scale xy plane flow patterns in our sealed samples which are preset by the geometry and defects and which could possibly play a role in creating regions showing different modes. In many of our samples "rosette" grids are (cf. text below) never formed.

²⁵E. Dubois-Violette, E. Guyon, and P. Pieranski, *Mol. Cryst. Liq. Cryst.* **26**, 193 (1973).

²⁶G. Durand, M. Veyssie, F. Rondelez, and L. Leger, *C. R. Acad. Sci.* **270**, 97 (1970).

²⁷If our explanation is correct, the formation of the branches backwards with respect to the movement, together with the mentioned relation between the polarity of the plates and the direction of motion, implies that the injected charge is negative.

²⁸The flow pattern might be similar to one of the above discussed dc low voltage a -type cell flow figures with a toroidal distribution of loop flows inside the bright round curves of photograph 3 Plate 1 and loops (complete this time) out of it.

²⁹P. Atten and J. C. Lacroix, *J. Mec.* **18**, 469 (1979).

³⁰W. S. Quon and E. Wiener-Avneer, *Solid State Commun.* **15**, 1761 (1974).

³¹P. Maneville, *Mol. Cryst. Liq. Cryst.* **70**, 223 (1981).

³²J. L. Janning, *Appl. Phys. Lett.* **21**, 173 (1972).